frontiers | Frontiers in Marine Science

TYPE Original Research
PUBLISHED 21 February 2023
DOI 10.3389/fmars.2023.1128855

OPEN ACCESS

EDITED BY
Jiapeng Wu,
Guangzhou University, China

REVIEWED BY
Shan Jiang,
East China Normal University, China
Ding He,
Hong Kong University of Science and Technology, Hong Kong SAR, China

*CORRESPONDENCE
Hannelore Waska
hannelore.waska@uol.de

SPECIALTY SECTION
This article was submitted to Marine Biogeochemistry, a section of the journal Frontiers in Marine Science

RECEIVED 21 December 2022
ACCEPTED 30 January 2023
PUBLISHED 21 February 2023

CITATION
Carvalho da Silva R, Seidel M, Dittmar T and Waska H (2023) Groundwater springs in the German Wadden Sea tidal flat: A fast-track terrestrial transfer route for nutrients and dissolved organic matter. *Front. Mar. Sci.* 10:1128855. doi: 10.3389/fmars.2023.1128855

Groundwater springs in the German Wadden Sea tidal flat: A fast-track terrestrial transfer route for nutrients and dissolved organic matter

Roger Carvalho da Silva[1], Michael Seidel[1], Thorsten Dittmar[1,2] and Hannelore Waska[1]*

[1]Institute for Chemistry and Biology of the Marine Environment (ICBM), Carl von Ossietzky University of Oldenburg, Oldenburg, Germany, [2]Helmholtz Institute for Functional Marine Biodiversity at the University of Oldenburg (HIFMB), Oldenburg, Germany

Submarine groundwater discharge (SGD) connects fresh groundwater and marine ecosystems and conveys terrestrially derived dissolved organic matter (DOM) and nutrients from land to sea. The connectivity of terrestrial and marine ecosystems *via* SGD depends strongly on local environmental settings. For example, SGD composition is modified on its transit through the coastal aquifer, with spring-type SGD from highly permeable aquifers presumably being less affected than diffuse discharge systems from sedimentary environments. In our study, we investigated spring-type SGD near Sahlenburg/Cuxhaven, Northern Germany, which passes through fine, unconsolidated tidal sediments before entering the coastal ocean. We characterized groundwater, surface water and seawater endmembers from different seasons and assessed the potential of tidal sediments impacting the biogeochemistry of "fast-track", point-source groundwater discharge systems. In addition to physicochemical parameters and nutrients, we analyzed the DOM molecular composition *via* ultrahigh-resolution mass spectrometry (FT-ICR-MS). Our data revealed a widespread physicochemical and geochemical influence of the groundwater springs on the tidal flat, producing low salinity and low dissolved organic carbon (DOC), and high nitrate and high oxygen concentrations not only in the springs, but also in adjacent porewater. From near- to offshore, salinity and DOC concentrations in springs decreased whereas nitrate and oxygen concentrations increased, resembling an inverse estuarine pattern. Furthermore, high nitrate values suggest anthropogenic sources (e.g., agricultural influence) in the surrounding watershed and may stimulate primary productivity in the tidal flat. Humic-like fluorescent DOM (FDOM) abundances and DOM molecular fingerprints indicated inputs of terrestrial DOM from nearshore saltmarsh plants, as well as from the nearby Elbe and Weser estuaries. Our study demonstrated that SGD had a strong geochemical impact even in the vicinity of large rivers, with productive springs actively hindering sulfate and nitrate reduction by flushing otherwise anoxic systems with oxygen. We posit that the geochemical influence

of groundwater springs in tidal flats is underestimated because it can extend far beyond their visual discharge points.

KEYWORDS

FT-ICR-MS, submarine groundwater discharge, subterranean estuary, groundwater springs, dissolved organic matter, tidal flat, North Sea

1 Introduction

Submarine groundwater discharge (SGD) occurs whenever hydrogeologic gradients allow the meteoric groundwater transport offshore (Povinec et al., 2008). In coastal aquifers, the mixing zone between the fresh groundwater and saline pore water is termed subterranean estuary (STE) (Moore, 1999). This term emphasizes the importance of mixing and biogeochemical reactions that modify both the terrestrial and marine endmember (Santos et al., 2008; Santos et al., 2021). Across the globe, porewater advection and SGD can enhance benthic fluxes of chemical constituents into the coastal water column, and often display distinct chemical, biological and physical properties (Kalbus et al, 2006; Santos et al., 2014). For example, the nutrient concentrations in groundwater can be much higher compared to (nearby) rivers or the coastal ocean and exhibit a different N:P stoichiometry (Slomp and Van Cappellen, 2004; Moore et al., 2006). In addition to nutrients, SGD can be enriched with dissolved organic and inorganic carbon (DOC and DIC) compared to seawater, acting as net source to the coastal ocean (Santos et al., 2008). In contrast to rivers and surface estuaries that are visible and whose contribution to the ocean is reasonably quantifiable, SGD is still poorly understood, since the water flow generally occurs below the surface and remains difficult to quantify (Kim, 2003). But in recent decades, the number of studies investigating SGD chemical composition and associated biogeochemical processes in the coastal ecosystem has increased considerably (Seeberg-Elverfeldt et al., 2005; Moosdorf and Oehler, 2017).

SGD mainly occurs in permeable sediments, where water diffusely seeps across the sediment-water interface (Povinec et al., 2008; Moosdorf et al., 2015), or as point-source discharge (Holliday et al., 2007) in the form of submarine springs. Diffuse SGD was reported for many types of shorelines globally, for example in the sandy beaches of the Gulf of Mexico (Santos et al., 2009) in permeable shelf sediments (Santos et al., 2012), in sandy intertidal flats (Santos et al., 2014), and sandy sediments in the Baltic Sea (Donis et al., 2017). Biogeochemical studies of porewater in high-energy beaches and tidal flats of the Wadden sea along the Northern German coast reported substantial release of nutrient-rich SGD, resulting in the increase of seawater nutrient concentrations in the study areas during low tide (Beck et al., 2008; Beck et al., 2017; Moore et al., 2011; Santos et al., 2015; Ahrens et al., 2020).

In contrast to diffuse SGD, submarine springs are a perceptible flow of water that is released through a natural opening in rock or soil (Toth, 1971). In regions with high aquifer permeability, submarine springs can discharge in single or multiple vents (Oehler et al., 2019a), and are frequently found in karstic regions (Moosdorf et al., 2015). Springs have been reported in many regions: Hawaii (Nelson et al., 2015), Indonesia (Oehler et al., 2018) and Florida (Luzius et al., 2018), to name a few. They have been identified as potential sources of nutrients (Carruthers et al., 2005; Null et al., 2014; Swarzenski et al., 2017; Oehler et al., 2019a) but their impact varies with seasonal changes in precipitation (Luzius et al., 2018). Overall, submarine springs reveal direct connections to the terrestrial watershed due to short residence times in the aquifer (Swarzenski et al., 2017).

Submarine springs may also occur in soft sediment habitats, for example intertidal sand flats (Zipperle and Reise, 2005; Röper et al., 2014), sand dune systems (Holliday et al., 2007) and muddy sediments at the subseafloor (Schlüter et al., 2004). To date, biogeochemical studies of such submarine springs are scarce. In general, spring water offers a unique opportunity to study a variety of underground processes: as groundwater flows through an aquifer, its composition integrates several geological and hydrological processes over large spatial areas and long periods of time, therefore providing valuable information about the adjacent watershed (Manga, 2001). However, the final transit of springs through unconsolidated sediments may affect their composition, and blur geochemical indicators of provenance, before they enter the coastal ocean.

The origins and fate of DOC and DOM in SGD have gained increased attention in recent years (Seidel et al., 2014; Webb et al., 2019; Waska et al., 2021). STEs are mixing zones of DOC from fresh groundwater and recirculating seawater, and this combination sustains a very active microbial reactor (Beck et al., 2017). Freshwater and marine DOM are often considered to be very diverse carbon reservoirs, their different chemical characteristics arising from differences in sources, turnover times, and turnover processes (Hedges et al., 1997; Repeta et al., 2002). The primary source of most DOM in the ocean is synthesis by algal and bacterial communities (Repeta et al., 2002; Koch et al., 2005). In contrast, the major source of DOM in freshwaters and coastal waters is derived from terrestrial vascular plant material which is degraded and transported through rivers, groundwater and estuaries to the sea (Stedmon et al., 2003; Longnecker and Kujawinski, 2011).

SGD can be an important source for DOC to coastal oceans (Goñi and Gardner, 2003; Santos et al., 2009; Smith and Cave, 2012; Szymczycha et al., 2014). However, groundwater DOM fluxes can be highly variable. For example, Seidel et al. (2014, 2015) found that SGD in the southern North Sea was enriched with both marine and terrestrial DOM, likely originating from the adjacent vegetation, benthic and planktonic primary production, and from organic detritus deposited on the sediment surface. However, Webb et al. (2019) showed that the groundwater fluxes in the saltmarsh and

mangroves may not necessarily represent a major source to surface waters. Depending on the surrounding terrestrial environment and hydrological regime, for example in systems with a strong DOM surface signal, the SGD-derived DOM signal may be masked. The residence time in the coastal aquifer also plays an important role: In comparison, diffuse SGD appears to have greater potential of accumulating DOC along its flow paths than spring-type SGD, mainly because longer residence times favor reducing conditions with lower abundances of electron acceptors, as well as additional release of DOM due to particulate organic matter degradation and desorption from mineral phases (e.g., Seidel et al., 2014; Nelson et al., 2015; Linkhorst et al., 2017). However, submarine springs can be seasonally or locally enriched with high concentrations of DOC (Luzius et al., 2018; Pain et al., 2019; Adyasari et al., 2021) which may discharge rapidly into the adjacent water column. Therefore, while SGD clearly is an important player that needs to be considered for management of freshwater resources and protection of coastal areas (Burnett et al., 2006), its impact on the organic carbon budget still needs to be better constrained, especially in regard to coastal carbon sequestration (Santos et al., 2021).

Even though the composition, sources, diagenesis, and preservation mechanisms of DOM are important for the global elementary cycles (Koch et al., 2005), the investigation of biogeochemical transformation processes remains a challenge. The complexity of the DOM molecular mixture is responsible for the difficulty in obtaining more knowledge in the composition and transformation of the organic matter (Schmidt et al., 2009). In addition, the low concentration of each individual compound, and the multiplicity of structural isomers for each molecular formula makes the analysis and interpretation a major challenge (Pohlabeln et al., 2017; Zark and Dittmar, 2018). Advancing analytical capabilities enable a more comprehensive understanding of the biogeochemical processes that control DOM composition (Steen et al., 2020; Wagner et al., 2020). To resolve the high chemical complexity and heterogeneity of DOM, electrospray ionization (ESI) coupled with Fourier-transform ion cyclotron resonance mass spectrometry (FT-ICR-MS) has demonstrated high potential (Nebbioso and Piccolo, 2013). With the use of FT-ICR-MS it is possible to obtain information on the exact elementary composition of the compounds in DOM (Kujawinski et al., 2004; Gonsior et al., 2009; Schmidt et al., 2009). FT-ICR-MS has been used previously to study Fe–DOM interactions (Linkhorst et al., 2017; Waska et al., 2021), identify origins of organic matter, and disentangle processing pathways in STEs (Seidel et al., 2015; Beck et al., 2017; Waska et al., 2021). In estuaries, it was used to differentiate DOM molecular composition along the salinity gradient (Osterholz et al., 2016). In groundwater, DOM displayed higher proportions of organic nitrogen and sulfur compounds compared to surface water DOM, which was linked to inputs from septic systems and rain events (Longnecker and Kujawinski, 2011).

At our study site, SGD occurs in the form of highly productive springs that discharge through tidal mudflats, with so far unknown effects on the local biogeochemistry (Figure 1). These springs, located in a North Sea tidal flat at Sahlenburg, Cuxhaven (Germany), were previously reported as having steep salinity and dissolved silicate gradients (Seeberg-Elverfeldt et al., 2005), indicating a persistent terrestrial influence on the nearshore marine environment. We applied FT-ICR-MS to analyze the DOM molecular composition from springs located in different regions of the intertidal mudflat, as well as seawater and groundwater endmembers, and linked the

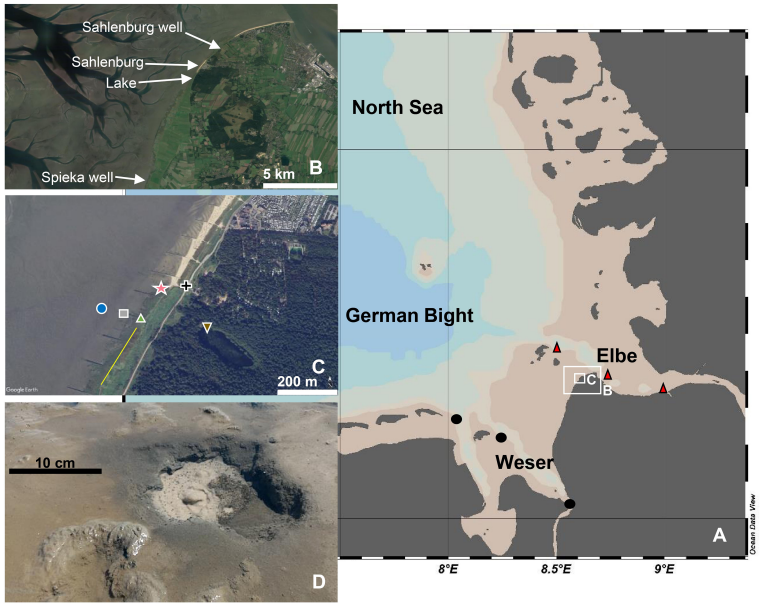

FIGURE 1
(A) Map of the German Bight with the Elbe and Weser estuaries. **(B)** Map of Sahlenburg, district of Cuxhaven, with sampling areas outlined by arrows. **(C)** Tidal flat area with spring locations and other sampled areas. **(D)** Groundwater spring ("sand boil") from Sahlenburg. The circle represents offshore, the square represents middle and the triangle represents nearshore springs, the inverted triangle represents the lake, the star represents the beach, and the cross represents water channel (ditch), respectively. The yellow line in **(C)** depicts the mean high water line. The map in **(A)** was made with Ocean Data View (Schlitzer, R., Ocean Data View, https://odv.awi.de, 2018), and the maps in **(B, C)** were made with Google Earth (©2016).

thousands of molecular formulae identified in the DOM pool to seasonal and spatial variations of tidal flat biogeochemistry. These patterns were used to elucidate and study the sources and potential transformation pathways of DOM on its underground land-sea transport. Specifically, our study addresses the following questions: Are the intertidal springs net sources of DOM to the coastal water column, and could this role change in different seasonal settings? Do the tidal flat sediments affect the DOM molecular composition of porewater as the springs pass through? Are the springs geochemically connected to tidal flat landmarks (such as saltmarshes) and/or other water bodies in the same watershed (e.g., lakes, groundwater wells, beach porewater)?

2 Materials and methods

2.1 Study area

Sahlenburg is a small village in the Cuxhaven district, in Lower Saxony, Germany, bordering the southern North Sea. It is located between the Weser and Elbe estuaries, which exert a strong freshwater influence in the region (Czitrom et al., 1988; Buth et al., 2015). This coastal zone of the northern part of Lower Saxony is particularly vulnerable to climate change, for example sea level rise (Sterr, 2008), and an overall increase of storm surges and numbers of storm tides in the German Bight (Danard et al., 2004). The region has relatively flat topography with some hills in the West and the South (Rahman et al., 2018). The watershed is characterized by a moraine consisting of buried valleys refilled with gravel, sand, silt, and clay that was formed by subglacial melt-water erosion during the quaternary glaciations. This structure is highly permeable and contains a large groundwater reservoir. Considering that the neighboring low-lying coastal regions are vulnerable to salt water intrusion, this watershed is particularly important for future supply of drinking water in the region (Steuer et al., 2009). The hydraulic connections to other groundwater reservoirs and the pathways for contaminants from the surface to deeper reservoirs can differ along their path because the filling of the buried valleys is not uniform. Consequently, saltwater intrusions into some groundwater reservoirs of the valleys may occur and this will be of increasing importance as the seawater level is expected to rise in the coming future, affecting the North Sea region (Piotrowski, 1994; Steuer et al., 2009).

2.2 Springs and intertidal zone

The Sahlenburg tidal flats are part of the Wadden Sea National Park of Lower Saxony, bordering the moraine to the Southeast and the Southern North Sea to the Northwest. The study site is relatively sheltered from waves and has a mean tidal range of 3.50 m (Schmidt et al., 2011). Sandy beaches and saltmarshes are located along the coastline, with the latter acting as accumulation sites for finer sediments. During high water, the salt marsh belt is partly submerged (Figure 1), while during low water, the tidal flat is exposed up to several km offshore due to the gentle slope of the coastline. In the intertidal zone of the study site, the glacial sands are overlain by Wadden Sea sediments which are depositions from the nearby Elbe estuary (Reineck and Siefert, 1980). In between, at 1-2 m depth below the sediment surface, a combined peat-clay layer is located which acts as an aquitard for the groundwater from the moraine watershed. Both peat and clay layer are thickest nearshore and thin out offshore (Rodemann et al., 2005), extending approximately 1 km seaward. Through cracks in the layer, meteoric groundwater discharges into the intertidal zone in the form of focused springs ("sand boils"), approximately 20 - 50 cm in diameter. In addition, larger-scale (up to meters) "pancake" structures were previously observed and attributed to broad upwelling of groundwater (Bartsch, 2009). Discharge from sand-boil type springs has been estimated to be ~ 700 L d^{-1}, with a seawater amount of <12%, for a single spring location (Schlüter and Maier, 2021). The multitude (at least 100) of springs commonly observed in the region (Bartsch, 2009), as well as potential diffusive fluxes, amount to substantial freshwater inputs into the local intertidal zone.

2.3 Sampling and *in situ* analyses

Field campaigns were carried out in June and August 2018, February 2019, November 2019, and July 2020. Porewater from the intertidal springs was sampled during low tide in three different types of locations in the tidal flat area (Figure 1): nearshore, where the springs were located close to the vegetated shoreline (saltmarsh), offshore, approximately 70 meters from the vegetation, and approximately in the middle between both locations. Spring water samples were taken from the surface (<10 cm), at 50 cm, and at 100 cm depth. For comparison, non-spring porewater from the tidal flat was collected from the same depths as spring water. In addition, porewater samples from a nearby sandy beach, and surface water (<20 cm depth) samples from a nearby lake were obtained. Seawater was sampled during high tide approximately 10 m offshore of the sandy beach in the vicinity of the lake location (Figure 1). Sandy beach porewater samples were collected at 50 cm, 100 cm, and 200 cm depth. Two regional groundwater wells were sampled, Spieka II Neufeld (Spieka well) and Sahlenburg III well 1 (Sahlenburg well) with approximately 8 kilometers and 3 kilometers distance respectively from the study area. Additionally, surface water samples were taken from 5 m depth from two rivers in the vicinity of Sahlenburg during the cruise HE527 of *RV* Heincke on March 2019. The Elbe and Weser River mouth sampling points were located at approximately 8 kilometers and 25 kilometers distance from the study area, respectively.

During the June and August 2018 campaigns, only spring porewater from the offshore zone was collected, since due to a very dry period, barely any springs were found. Beach porewater, lake water, and seawater were not sampled in June and August 2018. In November 2019 water samples from the two groundwater wells were collected, as well as meteoric water from a channel (ditch) next to an unpaved road adjacent to the sampling site. Tidal porewater was sampled only in February 2019 and July 2020.

At the sampling locations, porewater was drawn using pre-rinsed polyethylene (PE) syringes and stainless-steel push-point samplers. Temperature, salinity, and dissolved oxygen concentrations were measured with a Hach (HQ40D) multiparameter probe for the November 2019 and July 2020 campaigns. During June 2018,

August 2018, and February 2019 temperature and salinity were measured using a WTW Multi 3430 probe with a TetraCon 925 Conductivity Sensor, and dissolved oxygen was measured with a hand-held flow-through cell and attached temperature probe (FireStringGO2, Pyro Science). Dissolved oxygen saturations were converted to molar concentrations using salinity and temperature data (Garcia and Gordon, 1992). Fluorescent DOM (FDOM) was measured on site after sample filtration using an Aquafluor Handheld Fluorometer/Turbidimeter 8000-010 (Turner Designs). The instrument is pre-set to an excitation center-wavelength of 375 nm and an emission wavelength range >420 nm, which corresponds to Peak C/M (marine/aquatic humic-like, Stubbins et al., 2014). Concentrations were noted as relative fluorescence units (RFU) based on a quinine sulfate standard.

Sample water filtration was conducted using polypropylene (PP) inline filter holders equipped with a sandwich of 0.8/0.2 µm acid washed SUPOR filter membranes (Pall) which were directly connected to the syringes. For the determination of nutrients in the November 2019 and July 2020 campaigns, samples were filtered into 20 mL PE Zinsser vials and poisoned with mercury chloride (HgCl2). In the February 2019 campaign, samples were stored frozen, and in June and August 2018, no samples for nutrients were collected. For Fe (II) determination, 1 mL of filtered sample was pipetted into 2 mL Eppendorf safe-lock PP tubes pre-filled with 100 mL ferrozine solution. For DOC, TDN (total dissolved nitrogen) and DOM analyses, samples were filtered into acid-washed high-density polyethylene (HDPE) sample bottles. From each station, 60 mL sample volumes were collected. Filtered samples were acidified with suprapur HCl to pH 2. Seawater samples were collected during high tide from the nearshore surf zone using acid-washed polycarbonate (PC) bottles before filtration into 60 mL HDPE bottles. All samples were kept onsite in cooling boxes. They were all filtered in between porewater stations during the day and acidified at the end of each day.

2.4 Sampling and laboratory analyses

2.4.1 Nutrients, DOC, and TDN analyses

All analyses for nutrients were performed spectrophotometrically using a Multiscan GO Microplate Spectrophotometer (Thermo Scientific). Phosphate was determined according to the methods of Itaya and Ui (1966) for concentrations <2.1 µM and Laskov et al. (2007) for concentrations >2.1 µM. Dissolved silicate (Si) was analyzed spectrophotometrically according to Hansen and Koroleff (2007). Nitrate + Nitrite (NO_X), and nitrite (NO_2^-) were determined according to the methods after Schnetger and Lehners (2014) and Reckhardt et al. (2015). Fe(II) was measured spectrophotometrically according to Viollier et al. (2000). DOC and TDN were measured based on the high temperature catalytic oxidation (HTCO) method using a DOC Analyzer (Shimadzu TOC-VCPH) equipped with a TDN unit. Analytical precision and trueness were better than 5% and were tested with deep-sea reference material (provided by D. Hansell at the University of Miami, USA) and low carbon ultrapure water.

2.4.2 Molecular characterization of DOM

For DOM molecular analysis, 40 mL of acidified samples were desalted and concentrated by solid-phase extraction with 100 mg Bond Elut PPL cartridges following the protocol by Dittmar et al. (2008). Briefly, the cartridges were washed and conditioned with methanol and ultrapure water (UPW) acidified to pH 2 with suprapur HCl. After sample extraction, the cartridges were washed with acidified ultrapure water (pH 2) and dried with Argon gas. All samples were then eluted from the cartridges with Optima grade methanol (Fisher Scientific) into acid-washed, pre-combusted 4 mL glass vials and stored at −20°C in the freezer. The average extraction efficiency (based on DOC) was 72% ± 16%. Samples were analyzed on a 15 Tesla Bruker solariX XR FT-ICR-MS (Fourier transform ion cyclotron resonance mass spectrometer) equipped with an electrospray ionization (ESI) source and a HyStar autosampler. The samples were adjusted to 2.5 ppm DOC in a 1:1 methanol-UPW mixture and then measured in broadband ESI negative ionization mode. The mass spectra were internally calibrated with a list of known $C_xH_yO_z$ molecular formulae over the mass range in the samples. With this calibration procedure, a mass error of < 0.1 ppm was achieved. Instrument and process blanks were measured with methanol/ultrapure water 1:1 (*v/v*). Instrument assessment was done with an in–house standard from North Equatorial Pacific Intermediate Water (NEqPIW) collected near Hawaii (Natural Energy Laboratory of Hawaii Authority, NELHA) (Osterholz et al., 2014). Molecular formula attribution was done with the server-based tool ICBM-OCEAN described in Merder et al. (2020). A method detection limit (MDL) of 2.5 was chosen to eliminate instrumental noise based on Riedel and Dittmar (2014). Alignment of samples was done with the "Fast join" setting and a sample tolerance of 0.3 ppm. Recalibration was applied with the ICBM-OCEAN default elemental composition and a minimum signal-to-noise ratio (S/MDL) of 1. Molecular formula assignment was performed with a tolerance of 0.5 ppm in the mass to charge ratio (*m/z*) range of 100-1000. The range of the chemically possible molecular formulae of the elements were set to $C_{1-100}H_{2-200}O_{0-70}N_{0-4}S_{0-2}$ P_{0-1}. The N, S, P rule and the isotope verification were applied to exclude unlikely formulae. For DOM, the acquired mass cross tables were filtered by removing all isotopes (^{13}C, ^{18}O, ^{15}N, and ^{34}S), as well as all mass peaks with O/C ratios = 0 and ≥1 and H/C ratios > 2.5. Mass signal intensities were normalized for each sample by dividing single intensities by the total sum and multiplying them with 10 000. The weighed sums of molecular properties (e.g., elemental composition, compound group classification, AI_{mod}) were calculated based on the distribution of relative signal intensities in the mass spectrum. All assigned unique molecular formulae were grouped into distinct molecular groups based on their elemental ratios (aromatic, highly unsaturated, unsaturated, unsaturated with N and saturated; Waska et al., 2021). In addition, an aromaticity index (AI_{mod}) was calculated which is indicative of the C–C double-bond 'density' in a molecule characteristic for aromatic and condensed aromatic structures (Koch and Dittmar, 2016). Furthermore, two DOM molecular indices were used, a molecular degradation index (I_{DEG}), that is based on single mass peaks displaying significant correlations with $\Delta^{14}C$-based ages of DOM (Flerus et al., 2012). Comparatively higher I_{DEG} values generally correspond to a higher degree of DOM degradation. The terrestrial index (I_{Terr}) is another molecular proxy analogous to I_{DEG}, described by Medeiros et al. (2016), who correlated normalized intensity of FT ICR-MS peaks with bulk $\delta^{13}C$ SPE-DOC and salinity patterns in a surface estuary. Higher I_{Terr} ratios are the consequence of an increase of terrigenous molecular formulae in the DOM.

2.4.3 Statistical analyses

We assembled datasets of DOM molecular composition, molecular indices, and environmental parameters based on location/sample type and campaigns. With the normalized signal intensities of all identified DOM molecular formulae, environmental data, DOC, TDN, and nutrient concentrations as well as FDOM values, a principal coordinate analysis (PCoA) based on a Bray Curtis dissimilarity matrix was performed using the R statistical platform (R core team, 2022). Statistical analyses and plotting were done in R, using the packages *vegan*, *ggplot2*, *plyr*, and *corrplot* as described previously by Seidel et al. (2017).

3 Results

3.1 Physicochemical parameters

3.1.1 Salinity, temperature, and oxygen

Over the course of different sampling campaigns, intertidal spring samples collected in July 2020 had the highest average salinities (Supplementary Table 1). As for the temperature, the highest average values were found in the summer campaigns, not only in surface waters (e.g., lake and seawater) but also spring and pore water samples. O_2 had the highest average concentrations in June 2018 (Supplementary Table 1).

With regard to local spatial variations, amongst the springs, salinity was highest in the nearshore springs and lowest in the offshore springs (Supplementary Table 1). When comparing all endmembers, seawater had the highest average values for salinity and lake water the lowest (Figure 2A). Furthermore, lake water also had the lowest average temperatures, while middle spring samples had the highest average temperatures. For O_2, amongst spring samples the highest average concentrations were found in the middle springs and the lowest average concentrations in the nearshore springs (Supplementary Table 1). Comparing springs with all other areas, seawater had the highest average O_2 concentrations and beach porewater the lowest (Figure 2B). The two sampled groundwater wells had also low salinities, and comparatively lower O_2 concentrations and higher temperatures than the intertidal springs in the respective sampling campaign (November 2019) (Supplementary Table 1). Elbe and Weser estuary samples had higher salinity and lower temperature compared to the intertidal springs.

3.1.2 Nutrients

In the intertidal groundwater springs, the highest average concentrations of dissolved Si were observed in July 2020 and the lowest in February 2019 (Table 1). Phosphate and nitrite concentrations were highest in July 2020 and lowest in November 2019. Overall, we found comparatively low nitrite concentrations in all samples. Therefore, the dominant NO_x species by far was nitrate (Table 1). The average concentrations of NO_3^- were highest in November 2019 and lowest in February 2019. Furthermore, NO_x correlated almost 1:1 with TDN, with some exceptions in the February 2019 campaign where nutrient samples were stored frozen (Supplementary Figure 1). Highest average ammonium concentrations were observed in July (Table 1). Overall, Fe(II) concentrations were mostly below the limit of detection in June 2018, February 2019, and November 2019. In August 2018, the average Fe(II) concentrations in springs were detectable but low when compared to July 2020 (Supplementary Table 1). Highest average concentrations of TDN were found in February 2019 and the lowest observed in August 2018.

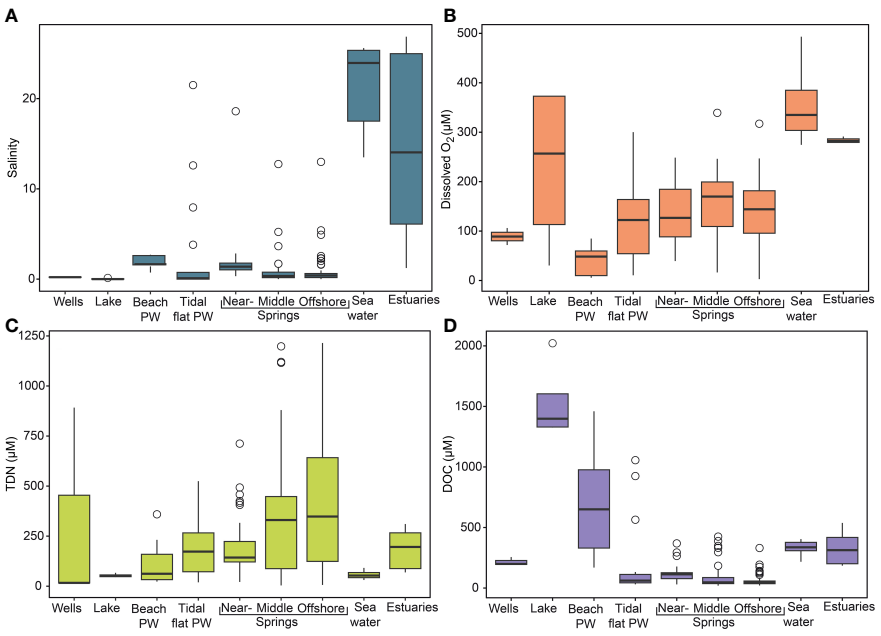

FIGURE 2
Physicochemical data for Sahlenburg tidal flat endmembers. **(A)** salinity, **(B)** oxygen concentrations, **(C)** TDN concentrations, **(D)** DOC concentrations. PW, porewater.

10.3389/fmars.2023.1128855

TABLE 1 Distribution of nutrients through the campaigns in the different locations.

Area/Sampling time	Si (µM)	PO_4^{3-} (µM)	NO_{2^-} (µM)	NH_{4^+} (µM)	NO_{3^-} (µM)
February 2019					
• Nearshore springs (5)	159.9±34.7*	0.6±0.5*	*b.d.**	b.d.*	**193.4±151.0***
• Middle springs (11)	71.5±48.2*	0.2±0.3*	0.1±0.2*	b.d.*	139.5±143.9*
• Offshore springs (18)	122.1±71.8*	1.4±2*	0.5±1.6*	b.d.*	148.7±108.1*
Beach porewater (3)	**221.3±115.5***	**8.7±13.4***	0.2±0.3*	**58±82***	*b.d.**
Tidal porewater (13)	61.4±80*	0.5±1.1*	0.1±0.1*	b.d.*	160.8±96.0*
Lake (2)	58.8±0.4*	*b.d.**	0.1±0*	b.d.*	0.5±0.6*
Seawater (4)	*54.5±29.4**	1.2±0.1*	2.2±0.9*	b.d.*	24.7±16.6*
March 2019					
Weser (3)	68.4±64.7	0.8±0.6	1.9±0	**6.7±1.4**	124.9±114.5
Elbe (3)	**125.8±55.9**	**1.4±0.5**	1.1±0.9	b.d.*	**247.8±106.2**
November 2019					
• Nearshore springs (25)	193±69.6	0.7±0.3	0.1±0.3	b.d.	194±148.5
• Middle springs (12)	**251.7±31.6**	0.6±0.8	b.d.	b.d.	377.6±61.4
• Offshore springs (25)	245.6±34.2	0.6±0.4	0.1±0.4	0.2±1.2	**607.1±349.4**
Beach porewater (2)	153±7.1	1.9±2.2	b.d.	7.5±10.6	b.d.
Lake (1)	*82.3*	0.3	b.d	b.d.	b.d.
Seawater (2)	71.2±6.9	1.4±0.4	b.d.	**17.7±4**	38.8±20.4
Sahlenburg Well (1)	191	b.d.	b.d.	b.d.	936
Spieka Well (2)	238±1.4	**29±0.3**	0.3±0.4	b.d.	b.d.
Water channel (1)	96.4	b.d.	**0.5**	b.d.	10.5
July 2020					
• Nearshore springs (21)	204.1±91.1	1.1±0.9	0.4±0.5	3.6±7.2	204.1±91.1
• Middle springs (23)	237.4±62.8	1.1±1	0.6±0.7	4.2±3.5	315.3±412.3
• Offshore springs (21)	258.3±59.6	1.9±2	0.8±1.4	*1.8±2.1*	**505±387.3**
Beach porewater (2)	**364.5±98.3**	**32±34.5**	**1±1.1**	**181.8±164.3**	13.7±4.7
Tidal porewater (5)	127.3±67.3	0.9±0.7	0.3±0.6	11±12.7	52.0±43.1
Lake (1)	91.1	*0.2*	0.8	3.3	5.9
Seawater (2)	*38.3±10*	3.9±1	*0.3±0*	6.4±1.5	*1.9±0.8*

For each campaign, maximum values are in bold, and minimum values are italic.
*Samples were frozen; b.d. = below detection limit. Numbers in brackets denote number of samples.

Amongst spring locations, average dissolved silicate and phosphate concentrations were highest in offshore and lowest in nearshore springs. But compared to all springs and other sample types, beach porewater had the highest dissolved silicate and phosphate concentrations (Table 1). Notably, NO_{3^-} and TDN concentrations were highest in offshore springs and lowest in lake water and beach porewater (Table 1 and Figure 2C). Ammonium had the highest average concentrations in the middle, and the lowest in the offshore springs. However, as with phosphate and silicate, beach porewater had the highest average ammonium concentrations when compared with springs and all other areas (Table 1). Regarding Fe(II) concentrations, the highest average concentrations were found in the middle compared to near- and offshore springs. Again, amongst all sample areas beach porewater had the highest average concentrations for Fe(II) (Supplementary Table 1). The Spieka well had higher average concentrations of silicate, phosphate and nitrite compared to the intertidal springs in the respective sampling campaign (November 2019) (Table 1).

In contrast, Sahlenburg well showed lower concentrations for silicate, and higher nitrate concentrations than intertidal springs. The Elbe had higher average concentrations for silicate and phosphate compared to intertidal springs, while on the other hand the Weser had lower concentrations for silicate (Table 1).

3.1.3 DOC and FDOM

DOC concentrations and FDOM intensities of the intertidal springs between campaigns were highest in July 2020 (Supplementary Table 1). In contrast, the lowest average concentrations of DOC were found in June 2018 and for FDOM in August 2018.

On a spatial scale, the average distributions of DOC concentrations had similar patterns as FDOM, with the highest values found in the nearshore and the lowest in the offshore intertidal springs (Supplementary Table 1 and Figure 2D). Comparing all endmembers, DOC concentrations increased in the order intertidal springs < tidal flat porewater < seawater < beach porewater < lake. FDOM intensities increased in the order intertidal springs < tidal flat porewater < seawater < lake < beach porewater. The two sampled groundwater wells had higher average DOC and FDOM values compared to intertidal springs in the respective sampling campaign (November 2019) (Supplementary Table 1). Elbe and Weser estuaries had higher average values of DOC and FDOM compared to the intertidal springs sampled in February 2019.

3.2 DOM molecular properties

3.2.1 General overview

A DOM molecular dataset with 8140 assigned molecular formulae was produced from a total of 221 samples (springs, porewater, seawater, lake, beach porewater, estuaries and water channel). The numbers of assigned molecular formulae per sample were highest in estuary (4575 ± 368) and seawater (3720 ± 665) samples, lowest in tidal flat porewater (2870 ± 848) and groundwater spring (2903 ± 233) samples, and in between for lake (3490 ± 142), well (3460 ± 1321), and beach porewater (3103 ± 388) samples. The identified peaks were in the mass over charge ratio (*m/z*) range between 101 to 891 Da, with weighted averages between 336 to 406.

Between campaigns, the weighted averages for *m/z* in spring samples were highest in February and November 2019, and the lowest in July 2020 (Supplementary Table 2). Highest weighted averages of H/C ratios were observed in June 2018 and the lowest in November 2019. The O/C ratios in February and November 2019 had the highest average values, while in August 2018 they were lowest. Highest averages of N/C ratios were found in November 2019 and July 2020, on the other hand the lowest ratios were found in the June 2018 campaign. AI_{mod} had the highest value in July 2020 and the lowest in June 2018 (Supplementary Table 2). A similar trend was observed for aromatic compounds (Supplementary Table 3). The DOM molecular compound groups of the intertidal springs were dominated by highly unsaturated compounds, with the highest percentage found in the February 2019 campaign. The saturated compounds had the lowest percentage in all campaigns except in June 2018. Here, the lowest average percentage was found for unsaturated compounds with N. Furthermore, unsaturated compounds with N had the highest percentage in July 2020 (Supplementary Table 3).

Amongst spring locations, across all campaigns, *m/z* values were highest in the middle springs, and on the other hand the lowest values were found in nearshore springs (Supplementary Table 2). Overall springs had higher average *m/z* values compared to other sample types, except for tidal flat porewater that had similar average *m/z* values as offshore springs (Figure 3A). In regard to the aromaticity index (AI_{mod}), amongst the springs the highest value was found in nearshore and the lowest in offshore springs. Overall, beach porewater and the groundwater wells had the highest AI_{mod} values compared to the other sample types (Figure 3B and Supplementary Figure 2). On the other hand, H/C ratios were highest in the offshore springs, while beach porewater had the lowest H/C ratios compared to all areas. The highest O/C ratios amongst springs were observed in the middle and the lowest in the offshore springs. Between all sample locations, the lake had the highest values for O/C ratios. Within spring areas, the highest N/C and S/C*1000 ratios were observed in nearshore springs. However, comparing all areas, seawater had the highest N/C and S/C*1000 ratios (Supplementary Tables 2, 3).

Highly unsaturated compounds were the dominant compound class in all sample types, increased from near- to offshore springs and had overall highest abundances in the springs compared to the other endmembers (Figure 3C). In line with elevated AI_{mod} values, the relative abundance of aromatic compounds was higher in nearshore compared to offshore and middle springs. However, beach porewater and well samples had the highest abundance of aromatic compounds overall (Supplementary Table 3 and Figure 3D). Note that amongst groundwater wells, aromaticity was 3-fold higher in Spieka compared to Sahlenburg Well (Supplementary Figure 2). Furthermore, saturated compounds were the least abundant compound group in the spring samples. Regarding all sample types, offshore springs and tidal flat porewater had the highest percentage for saturated compounds. Unsaturated compounds with N had highest relative abundances in offshore spring and seawater samples (Supplementary Table 3).

The two sampled groundwater wells had higher AI_{mod} values and aromatic compounds, and correspondingly lower H/C ratios, compared to the intertidal springs in the respective sampling campaign (November 2019) (Supplementary Tables 2). Furthermore, the two groundwater wells had lower relative abundance of unsaturated compounds, unsaturated compounds with N and saturated compounds compared to the intertidal springs (Supplementary Table 3 and Supplementary Tables 2).

Elbe and Weser estuaries had higher O/C, N/C and S/C*1000 ratios but lower H/C ratios compared to the intertidal springs (Supplementary Table 2). Furthermore, the two estuaries had higher relative abundances of aromatic compounds and intensity weighted averages of AI_{mod} compared to the intertidal springs (Supplementary Tables 2, 3; Figure 3 and Supplementary Figure 2).

3.2.2 Statistical results

To investigate the processes related to changes in the molecular DOM composition in our study, we conducted a principal coordinate analysis (PCoA). First, the DOM molecular composition data of all samples were used to calculate a Bray-Curtis dissimilarity matrix. The resulting coordinates were then correlated with environmental parameters (salinity, temperature, TDN, DOC, FDOM) as well as DOM chemical properties (e.g., elemental ratios, compound groups) gained from weighed averages of the molecular fingerprints of the samples (Waska et al., 2021). The first two PC (principal coordinate) axes combined explained 62% of the DOM molecular variability (Figure 4). Clear molecular clusters were identified, notably a separation between offshore and nearshore springs along PC1 which explained 48% of total molecular variability among sample

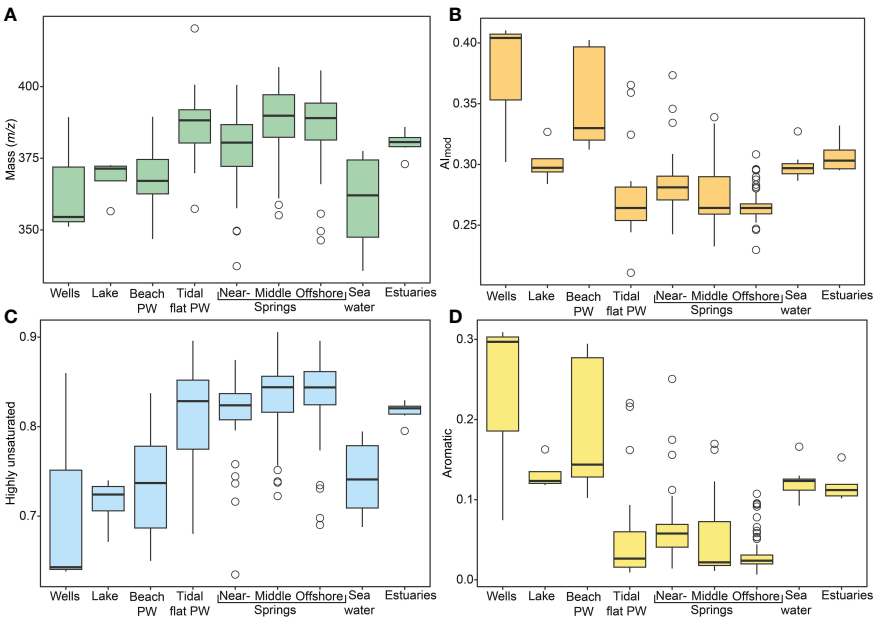

FIGURE 3
DOM molecular data for Sahlenburg tidal flat endmembers. **(A)** *m/z*, **(B)** AI_{mod}, **(C)** intensity-weighted relative abundance of highly unsaturated compounds, and **(D)** aromatic compounds. PW, porewater.

distribution. Middle springs and tidal flat porewater did not show a clear trend but instead were distributed among offshore and nearshore springs. Furthermore, PC1 was correlated negatively to conductivity, DOC concentrations, FDOM fluorescence, AI_{mod} and relative abundances of aromatic compounds, and positively to TDN concentrations. PC2 explained 14% and was related to abundances of molecular groups of unsaturated compounds with N, unsaturated, saturated DOM groups, and O/C ratios. Overall, elevated DOC and FDOM concentrations, aromatic compound abundances, and AI_{mod} values were associated with nearshore springs, seawater, beach porewater, lake water, and groundwater wells. On the other hand, elevated abundances of unsaturated, unsaturated with N, and saturated compound groups were associated with the offshore springs. Additionally, offshore springs were related to high TDN concentrations and higher H/C ratios.

A second PCoA with intertidal springs and endmember samples (February 2019) together with surface water samples from Elbe and Weser estuaries (March 2019) was conducted which overall showed similar trends with the first PCoA (Figure 5).

The first two PC axes explained 73% of the DOM molecular variability. Again, we observed a separation between nearshore and offshore spring samples, and a slightly higher similarity of nearshore spring samples with lake, beach porewater, seawater and estuarine samples regarding DOM composition. Both estuaries clustered very close together, and tidal flat samples clustered close to offshore springs. PC1 explained 66% of DOM variability and was significantly negatively correlated with salinity, DOC and FDOM concentrations, AI_{mod} and relative abundances of aromatic compounds. It was significantly positively correlated with intensity-weighed H/C ratios and TDN concentrations. PC2 explained 7% and

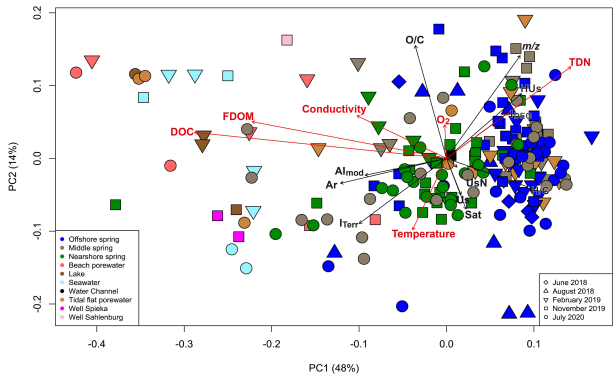

FIGURE 4
Principal coordinate analysis (PCoA) from all samples across the campaigns based on Bray-Curtis dissimilarities of the relative abundance of FT-ICR-MS derived molecular formulae data. The percentages give the DOM molecular variability as explained by the PC1 and PC2 axes. Correlations of coordinates to molecular characteristics and environmental parameters were considered significant with $p \leq 0.05$. Colors represent the sample types and symbols represent sampling campaigns.

was positively correlated to relative abundances of unsaturated, saturated, and unsaturated with N compounds and negatively correlated to relative abundances of highly unsaturated and with intensity-weighed O/C ratios.

Spearman correlations were conducted with physicochemical parameters and DOM from intertidal springs across the campaigns ($p < 0.05$, n=174) (Figure 6). In line with the results from the PCoAs, DOC concentrations were positively correlated with FDOM values and salinity, and on the other hand negatively correlated with TDN concentrations. The correlation matrix also revealed a significant decrease in salinity and DOC with increasing spring sampling depths. Moreover, spring temperature was significantly positively correlated with salinity and DOC concentrations, and significantly negatively correlated with TDN and oxygen concentrations, confirming a trend visible across all sample types in Figure 4 (directions of red arrows). H/C ratios were significantly negatively correlated with DOC and FDOM concentrations, as well as AI_{mod}, but were significantly positively correlated with unsaturated N-containing compounds.

Analogous to surface estuaries, we explored the quantitative and qualitative characteristics of DOM along the regional land-ocean gradient, by plotting DOC concentrations and the molecular degradation index I_{DEG} against salinity (Supplementary Figure 3). Assuming the Sahlenburg and Spieka wells as watershed groundwater endmembers, and seawater with salinity ~25 as marine endmember, most spring and tidal flat data points were either aggregated in the vicinity of the groundwater endmember or scattered around the mixing line with some positive deviations in the case of DOC concentrations, and negative deviations in the case of I_{DEG} values.

4 Discussion

4.1 Spatial and seasonal trends of physicochemical parameters

The overall low salinities in springs, beach porewater, and tidal flat porewater (<10) compared to seawater (>20) reflect a strong contribution of fresh groundwater in the whole tidal flat area. Overall, seawater salinities in this region of the German Bight are in the brackish range (~18-24) due to freshwater input from the Elbe River (Brase et al., 2017). Among the three spring location types, the lowest salinities were found offshore, and the highest nearshore (Supplementary Table 1). One explanation for this pattern could be local topographic heterogeneity: There was a systematic difference in spring sizes; nearshore springs were usually smaller (diameter ~2-4 cm) and comprised of groups (3-7 springs in clusters), compared to offshore springs (diameter ~5-30 cm, single springs). Furthermore, nearshore springs were located near the high water line and in depressions in the tidal flat relief, which may have favored seawater retention in pools during low tide, as well as addition of recirculating seawater. Another explanation could be the local hydrology: We did not find any springs much further offshore than our "offshore" locations (i.e., ~ 70 m from the salt marsh), in line with an earlier report on most springs being typically located between 25 m and 90 m into the tidal flat (Bartsch, 2009). Considering that the offshore springs were downslope of the nearshore springs, and towards a thinning peat-clay layer, this could indicate that the former is subject to stronger hydraulic gradients and possibly under a weaker confining layer to break through than the latter.

Regardless of spring location, spring salinities in our study were comparatively low and in the low range of freshwater springs from another North German intertidal sand flat in Sylt, Germany (0-16; Zipperle and Reise, 2005). Generally, intertidal spring systems, even those occurring in unconsolidated sediments, appear to be characterized by lower salinities compared to diffuse groundwater discharge systems, which range from brackish to even hypersaline (10-37; Hays and Ullman, 2007; Waska and Kim, 2010; Ahrens et al., 2020). The high hydraulic pressure of these – at least partially – confined aquifer systems seems to effectively prevent substantial seawater intrusion.

The seasonal patterns in spring salinity (Supplementary Table 1) did not co-vary consistently with precipitation rates during the campaigns, which were highest in November 2019 (76-100 mm) and July 2020 (101-125 mm) and lowest in June 2018 and February

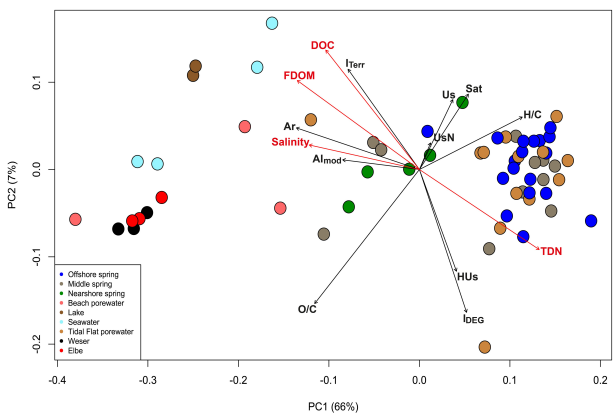

FIGURE 5
Principal coordinate analysis (PCoA) from February 2019 samples together with Weser and Elbe estuary samples from March 2019 based on Bray-Curtis dissimilarities of the relative abundance of FT-ICR-MS derived molecular formulae data. The percentages give the DOM molecular variability as explained by the PC1 and PC2 axes. Correlations of coordinates to molecular characteristics and environmental parameters were considered significant with $p \leq 0.05$. Colors represent the sample types.

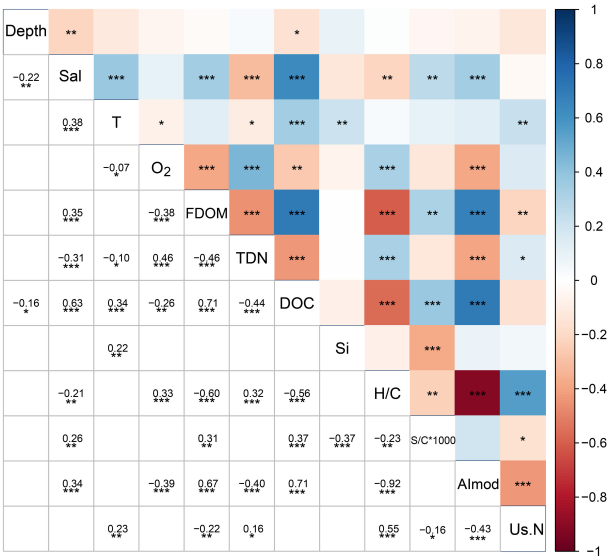

FIGURE 6
Spearman correlation between physicochemical parameters and DOM from intertidal springs across campaigns ($p < 0.05$, n=174). The red color represents negative correlations and the blue color represents positive correlations, and the color shades are representative of the correlation coefficient (Spearman's ρ). Asterisks indicate significance of correlation at the <0.05 (*), <0.01 (**) and <0.001 (***) levels. Us.N indicate unsaturated compounds with nitrogen. S/C*1000 is the molecular sulfur-to-carbon ratio multiplied by 1000.

2019 (31-40 mm, Deutscher Wetterdienst). Thus, despite the overall low salinities in the tidal flat, which were clearly groundwater-driven, it appears that precipitation had no direct influence on the salinity of the springs. Central Europe including our study site experienced a severe drought period from spring to fall 2018 with overall low rainfalls and high temperatures compared to previous decades (Ionita and Nagavciuc, 2020). Subsequently, we observed lower occurrences of intertidal springs in June and August 2018. Especially, small-scale nearshore springs could not be found, and mostly offshore springs were sampled in these two first campaigns. Despite these extraordinary conditions, the spring biogeochemistry was similar to the other sampled seasons, and even the average temperature was not significantly higher than for example in June 2020. Overall, the weak seasonal trends in spring physico-chemistry were surprising considering the strong temperature oscillations (~8-20°C) which we expected to impact microbial activities. Spring temperatures were weakly negatively correlated with oxygen and TDN (i.e., NO_x) concentrations (Figure 6) and the only two spring samples containing measurable Fe(II) concentrations were collected in the summer campaigns (Supplementary Table 1), indicating enhanced respiration rates. However, DOC concentrations in the groundwater springs were rather low and may not provide enough substrate for the local microbial communities.

FDOM was used as an SGD tracer in coastal environments in previous studies (Kim et al., 2012; Nelson et al., 2015; Kim and Kim, 2017) and in addition applied to differentiate for example terrestrial, anthropogenic or microbial sources of DOM. The handheld device used in this study has emission and excitation spectra targeting mainly terrestrial, "humic-like" FDOM fractions (Coble, 1996). Therefore, our findings suggest that FDOM in the tidal flat could be from terrestrial sources, albeit not necessarily from the meteoric groundwater. The elevated values in nearshore springs might be from saltmarsh plants, but it is also feasible that finer sediments with particulate organic carbon from the nearby rivers preferentially settle in these marshes. In addition, the sediments of the region are characterized by buried Pleistocene marsh peats (Streif, 2002) and their degradation can lead to the discharge of terrestrial FDOM through the springs and porewater in the tidal flats. Indeed, the peat-clay layer was reported as being most extensive nearshore (Bartsch, 2009). Similarly, transport of peat-derived DOM through SGD was also suggested for a barrier island near our study region (Waska et al., 2021).

Overall, our findings suggest that the intertidal groundwater springs in Sahlenburg are not a major source of DOC and FDOM to the local coastal ocean: DOC concentrations in the springs and porewater overall were much lower than reported from diffuse-type systems (e.g. an intertidal creek bank and a sheltered sandy beach, 100 – 2700 µM, Seidel et al., 2014; Seidel et al., 2015) and large tidal flats (60 – 1700 µM, Kim et al., 2012) and in a similar range in a karstic system (40 – 85 µM, Tamborski et al., 2020). Even the nearby groundwater wells in Sahlenburg and Spieka had up to fourfold higher DOC concentrations than e.g. the offshore springs (Supplementary Table 1). Slightly higher average values of DOC and FDOM in the nearshore springs, together with higher salinities compared to offshore samples, could be rather explained by local effects, such as the input of marine DOM from seawater, either surficial or after recirculation through the saltmarsh, or possibly peat leachates. Unpublished tritium-helium dating results (Schlüter pers. comm.) have indicated that this groundwater is decades old, which could mean that DOM has already undergone substantial microbial degradation. Another explanation for the low DOC concentrations in the springs compared to wells or nearby surface waters could be removal *via* adsorption to minerals in the aquifer (Shen et al., 2015). In contrast, the fine-grained intertidal sediments did not appear to

contribute much to DOC production or removal in the springs during their final flow path before discharge, although some mid-salinity concentrations appeared to be higher than expected from the groundwater-seawater mixing curve (Supplementary Figure 3A). Perhaps high groundwater velocities resulted in shorter contact times with the sediment matrix, allowing for less time for exchange processes resulting in low concentrations in the springs (Tiemeyer et al., 2017). In support of this argument, we observed strong bubbling ("sand boils") during the sampling campaign, indicating high fluxes from the springs. Previously, discharge rates of more than 700 mL min^{-1} were observed in springs from our study region by Schlüter and Maier (2021) with a released groundwater volume of about 400 L in 7h. In support of this suggestion, some tidal flat and especially the beach porewater samples, presumably subject to longer water residence times, displayed much higher DOC concentrations than expected based on the local groundwater sources (Supplementary Figure 3A). Initially, a detailed description of the beach subterranean estuary was not our major research objective, but its extraordinary biogeochemistry clearly warrants a more comprehensive investigation in future studies.

TDN concentrations in the springs in Sahlenburg were at the high end of reported sites under anthropogenic influence. For example, TDN concentrations ranged from 67 – 158 µM in a diffuse estuarine intertidal flat system (Santos et al., 2014) and 51.9 – 148 µM in volcanic submarine springs (Swarzenski et al., 2017). The much higher concentrations of TDN (here essentially comprised of nitrate) in the intertidal springs compared to those found in the seawater and nearby rivers suggest that they are an important source of nitrogen to the surrounding tidal flat area. To illustrate, Schlüter and Maier (2021) estimated a maximum groundwater discharge volume of 1371 L d^{-1} for one "sand boil" in Sahlenburg. Using this volumetric flux, the average TDN and Si concentrations of all sampled springs and seasons in our study would yield inputs of 447 mmol TDN d^{-1} and 279 mmol Si d^{-1} for only a single groundwater point-discharge site. Note that although we did not quantify spring abundances in this study, our observations as well as previous reports indicate the occurrence of at least one point-source discharge per m shoreline (Bartsch, 2009). In comparison, Ahrens et al. (2020) estimated a maximum DIN flux of 102 mmol d m $shoreline^{-1}$ for the subterranean estuary of a barrier island high-energy beach, approximately 40 km west of our study site.

High values of nitrogen and especially nitrate are typically observed in watersheds close to agricultural, artificially fertilized land and shallow groundwater below sewage plumes (Jordan et al., 1997, Slomp and Van Cappellen, 2004). The high values found for nitrite and nitrate in the intertidal springs were similar to those from an SGD site in the vicinity of a watershed impacted by agriculture that ranged from 0.02 µM to 460 µM for NO_x (nitrite and nitrate) (Bishop et al., 2017). Furthermore, the high concentrations of nitrate in the intertidal springs suggest a shallow groundwater source since nitrate sources occur on or near the soil surface. Like most parts of Northern Germany, the Sahlenburg area is extensively used by agriculture with chronically high nitrate concentrations particularly in the shallow groundwater as documented by local authorities (Klages et al., 2022) and evidenced by our data from the Sahlenburg monitoring well (Supplementary Table 1). In the Sahlenburg springs, the high average concentrations of nitrate, and lower concentrations of nitrite and ammonium are indicative of an oxygenated system where there is little denitrification (Tamborski et al., 2020), in line with elevated dissolved oxygen concentrations. Additional upstream aspects could impact the nitrogen concentrations in the intertidal springs, such as the time from infiltration and exfiltration of nitrogen loading to the land surface, the proximity of nitrogen sources to the springs, and local climatic variations (Toth and Katz, 2006). For example, at the dune base of a high energy sandy beach, enrichment of groundwater with nitrate was linked to nitrification of remineralized ammonium (Ahrens et al., 2020).

In addition to the high NO_3^- concentrations, our observed high concentrations of dissolved oxygen, which were close to saturation, suggest that the spring groundwater does not originate from a deep aquifer, or at least is in contact with the vadose zone before it reaches the tidal flat. It is also noteworthy in this context that while spring geochemistry did not exhibit distinct seasonal trends, the temperature of the spring water fluctuated highly depending on ambient air conditions. The high oxygen concentrations and fast discharge rates led to low iron concentrations in springs and tidal flat porewater compared to beach porewater, although the tidal flat is comprised of fine-grained sediments and would normally be dominated by sulfate reduction (Seidel et al., 2014), while beach STEs are generally more oxic- to suboxic (e.g. Ahrens et al., 2021). Therefore, we propose that the spring groundwater is exposed to the atmosphere before it enters the tidal flat and does not spend enough time in the tidal flat sediments to become anoxic again.

The observed enrichment of silicate in springs and beach porewater compared to seawater was expected because typically, groundwater is enriched in dissolved silicate compared to surface waters. Thus, dissolved silicate is used to trace groundwater transport processes in the sediment and the coastal aquifer and can complement other conventionally applied tracers, such as radon or radium (Oehler et al., 2019b). Additionally, the higher concentrations of silicate in the intertidal springs and beach porewater compared to the other sampled areas can be linked to the dissolution of biogenic silicate derived from sedimented diatoms, which can be a significant organic matter source for the *in situ* active microbes (Seidel et al., 2014). Our results were in the high end of ranges when compared with other studies: for example karstic coastal springs in the Mediterranean ranged from 36.2 to 90.3 µM (Garcia-Solsona et al., 2010). In a high-energy beach and a back barrier tidal flat concentrations up to 320 µM were linked to inflow of fresh/brackish groundwater from below, and in porewaters of the tidal flat higher concentrations of silicate were associated with high deposition rates and advective porewater circulation, contributing to the incorporation and subsequent dissolution of biogenic opal (Reckhardt et al., 2015).

Lower concentrations of dissolved phosphate were likely an additional result of the oxic conditions, as phosphate is removed through sorption onto minerals such as oxides of Fe, Al, and Ca, and co-precipitation (Welskel and Howes, 1992; Slomp and Van Cappellen, 2004). Our intertidal springs had higher average concentrations than those in submarine karstic springs at northwest Mediterranean Sea, which ranged 0.15 – 0.46 µM (Tamborski et al., 2020), and higher than those in a diffuse seepage nearshore system

with average values of 2.3 µM, and ranging from nearly 0 – 12 µM (Santos et al., 2008). Nevertheless, groundwater springs were depleted compared to surface seawater, and despite nearby agriculture, groundwater phosphate was not a major source due to the prevailing oxic conditions. On the other hand, sub- to anoxic beach porewater may contribute excess phosphate to the coastal ocean (Table 1).

4.2 Spatial and seasonal trends of the molecular DOM composition

We did not find a distinct seasonal trend in DOM geochemistry of the intertidal springs from Sahlenburg through our data displayed in the PCoAs (Figures 4, 5). Likewise, spatial patterns of local DOM sources were very heterogeneous. Nevertheless, molecular characteristics of DOM in intertidal springs were distinct from those in seawater and other endmembers. These observations indicate that spatial trends are far more relevant than seasonality for DOM molecular composition in the Sahlenburg groundwater springs. Overall, the land-ocean gradient in Sahlenburg is spatially complex; for example, the nearshore springs were more similar to seawater in their DOM composition than the offshore springs. Furthermore, the tidal flat porewater had similar salinity and molecular composition to the springs, implying that, rather than springs providing terrestrial geochemical "islands" in a marine environment, the whole tidal flat appears to be strongly saturated with meteoric groundwater. Interestingly, the water channel (meteoric water from a ditch) had a DOM composition similar to nearshore spring samples (Figure 4). The sampling location for the water channel was in a vegetation zone near the saltmarsh around ~300 m from the sampling zone. Either this sample was impacted by the same vascular plant-derived inputs, or it was in contact with the groundwater that later discharged into the nearshore springs. Furthermore, the DOM molecular similarities, as well as the slightly elevated salinities, imply that the nearshore springs had not only an imprint from the local vegetation but also from the seawater. Likewise, DOM in the middle springs and tidal flat porewater was likely a mixture of DOM derived from groundwater springs and seawater.

Aromatic DOM compound abundances and AI_{mod} were elevated in nearshore springs, seawater, and terrestrial endmembers (wells, channel, and lake), compared to offshore groundwater springs, indicating relatively higher amounts of terrestrial DOM in the former compared to the latter. Indeed, AI_{mod} generally is related to terrestrial DOM derived from degradation of polyphenolic land-derived compounds such as lignin and tannin (Seidel et al., 2017). This could also explain the higher aromaticity in nearshore springs, and the decrease towards offshore spring locations. Surprisingly, seawater had elevated levels in aromaticity and FDOM and thus molecular similarities with the terrestrial endmembers in our study, such as lake water and inland wells. In surface estuaries, generally negative correlations are observed between aromaticity and salinity (Osterholz et al., 2016). But in our study, we observed positive correlations between AI_{mod}, FDOM, and salinity. This, as well as its overall low average salinity (~14 – 26), suggests that our seawater endmember was influenced by terrestrial DOM from the two adjacent large Weser and Elbe rivers. Concurrently, a relatively high I_{Terr} index, indicative of a terrigenous signature (Medeiros et al., 2016), was observed in the seawater compared to the springs (Supplementary Table 2). Finally, for the February and March 2019 campaigns, DOM of the two estuaries had a similar molecular composition as seawater (Figure 5). These results further support our observation that seawater is strongly influenced by these estuaries in the area. Nevertheless, some seawater samples formed an additional cluster separated from the estuaries, in the vicinity of beach porewater and lake samples. As the seawater samples were always collected at high tide, directly offshore from the beach porewater and lake locations, we suggest that local heterogeneities in wind- and tidally driven currents may be responsible for these distinct patterns. Furthermore, higher molecular S/C ratios of DOM in seawater and estuaries compared to springs and porewater from Sahlenburg could be related to anthropogenic sources in the estuaries, as well as resuspension of anoxic (sulfidic) estuarine sediments and release of porewater with sulfur-enriched DOM into the water column from surrounding tidal flats along the German coast (Seidel et al., 2014).

The lower molecular mass of DOM in seawater compared to springs could result from microbial degradation, as previously reported from FT-ICR-MS studies of terrestrial and marine DOM exposed to microbial activity (Burdige and Gardner, 1998; Kim et al., 2006). These trends in DOM molecular mass also apply to porewater and seawater from a different intertidal flat area near our study site (Seidel et al., 2014). DOM in beach porewater, seawater and lake water had lower molecular masses and was more oxidized as indicated by higher O/C ratios compared to intertidal springs. DOM in the offshore springs had also higher H/C ratios and as such more aliphatic character than DOM at all other sites. In previous studies high H/C ratios in submarine springs were associated with labile DOM produced autochthonously in the aquifer, or through microbial transformation of vascular-plant-derived DOM during infiltration from the soil, increasing the abundance of aliphatic DOM (Adyasari et al., 2021). Furthermore, selective adsorption of aromatic, oxygen-rich DOM to aquifer minerals may result in higher H/C ratios, and lower O/C ratios in DOM in groundwater (Shen et al., 2015). Contrastingly, the lower H/C ratios in DOM of our beach porewater compared to the seawater were in line with patterns found in the STE of a high energy beach, and possibly due to iron oxidation-reduction cycles which cause enrichment with humic-like FDOM and aromatic compounds (Waska et al., 2021).

Despite the slightly higher H/C ratios, which are generally associated with higher lability (D'Andrilli et al., 2015), offshore groundwater also had the highest molecular degradation index I_{DEG}, as well as highest abundances of highly unsaturated compounds amongst all sample types (Figure 3C; Supplementary Table 2; Supplementary Figure 3B; Flerus et al., 2012), pointing to an extensive DOM turnover in the coastal aquifer. Our results indicate that the use of H/C ratios as an indicator for "freshness" (i.e., recent primary production) or lability (i.e., suitability as a substrate for microbial metabolism) must be evaluated in the environmental context, and ideally together with several other molecular markers. Indeed, the concurrent increase of I_{DEG} and highly unsaturated

compounds suggest increasing amounts of reworked DOM (Adyasari et al., 2021). An overall increase of the relative contribution of highly unsaturated compounds from nearshore to offshore springs, together with an increase of I_{DEG} from lower to higher degradation state, implies that DOM was actively utilized during transport in the STE (Adyasari et al., 2021). Still, DOC concentrations in spring samples were overall very low. An advanced DOM degradation state, together with overall low DOC concentrations, could explain low aquifer reactivities, preventing the complete exhaustion of oxygen and nitrate along the groundwater flow paths. Previously, Montiel et al. (2019) proposed that organic(peat-)rich subterranean estuaries enhanced denitrification of groundwater from anthropogenically impacted watersheds, while increasing ammonium and dissolved organic nitrogen loads to the coastal water column. Although peat layers are common in North Germany and partially comprise the confined layer in our study site, they appeared to have only a slight impact on DOC concentrations and DOM composition. Instead, the low-DOC, high-I_{DEG} spring DOM characteristics resembled those of deep-sea DOM (Flerus et al., 2012), which is generally considered as having low reactivity. Furthermore, the groundwater spring samples had a relatively high number of assigned DOM molecular formulae considering their very low DOC concentrations. For comparison, spring samples had approximately 30% less molecular formulae than seawater at > threefold lower DOC concentrations, indicating that the concentrations of single organic compounds in the springs may have been much more diluted than in any other investigated sample type. High DOM molecular complexity in low overall DOC quantities can limit microbial substrate utilization (Dittmar et al., 2021). Under these circumstances, the capacity of the coastal aquifer to mitigate nitrogen pollution *via* denitrification could be hampered, resulting in the high nitrate loads of discharging groundwater.

We observed different patterns in regard to the distributions of organic and inorganic nitrogen species: The relative abundances of unsaturated DOM compounds with N were highest in offshore springs and showed similar trends as TDN concentrations. This suggests similar sources, since, for example, elevated nitrate concentrations but also unsaturated DOM compounds with N have been related to anthropogenic land use, agriculture and urbanization (Slomp and Van Cappellen, 2004; Roebuck et al, 2019). However, the intensity-weighed molecular N/C ratios indicated that seawater had overall more N-containing formulae while aliphatic DOM compounds with N were more prominent in groundwater. This is probably because seawater contains more phytoplankton-derived DOM that is more enriched in N-containing aliphatic compounds compared to terrigenous DOM, which in turn has overall lower N/C ratios (Seidel et al., 2017). Nonetheless, SGD has been identified as important pathways for the transport of anthropogenically sourced nutrients to coastal oceans (Santos et al., 2021). Our study shows that point-source groundwater discharge systems have the potential of being a "fast-track" transport system for anthropogenic nutrients and DOM impacting the local biogeochemistry of tidal systems. For future work, linking N-containing DOM compounds with other pollution tracers such as stable nitrogen isotopes could be a worthwhile future exploration of the organic nitrogen pool in Sahlenburg groundwater.

5 Conclusions

We explored the DOM molecular composition and transformations in groundwater springs of an intertidal flat area. In our study site, chemical parameters and DOM compounds of springs showed a high spatial heterogeneity. Even though the discharging groundwater originated from a shallow aquifer as indicated by physicochemical properties, nutrient concentrations, DOM composition and other groundwater properties did not vary seasonally. Nearshore springs received inputs of vascular plant-derived, aromatic DOM. Offshore springs, on the other hand, were depleted in aromatic DOM, while seawater carried terrigenous DOM from the nearby rivers into the tidal flat. Furthermore, the offshore springs were influenced by anthropogenic activity manly from agricultural land use, as suggested by high TDN concentrations and the abundance of unsaturated N-containing DOM molecular formulae.

Overall, we posit that in this system, even fast discharge springs can be influenced by biogeochemical processes in the sediments. The groundwater springs in Sahlenburg were locally distinct, possibly due to different residence times, heterogeneity of sediment layers, vicinity of vegetation, and spring size. Nevertheless, they exerted an overall strong, regional geochemical influence on the tidal flat, creating an oxygenated, nitrogen-enriched, organic-poor aqueous subspace in an otherwise organic-rich environment dominated by sulfate reduction. Our study stresses the importance of considering SGD fluxes of point-source groundwater discharge systems in soft-bottom habitats because they have the potential of transporting (anthropogenically derived) carbon and nutrients on a "fast-track" from land to coastal oceans. In rivers, the pulse-shunt concept describes seasonal changes in water residence times which impact DOM processing along the flowpath (Raymond et al., 2016). Taking this concept to the Sahlenburg groundwater springs, they could represent spatial pulse-shunt systems where flow is slow in the watershed but accelerates upon discharge from the confined coastal aquifer into the intertidal zone. The hydrology and resulting geochemistry of a complex hydrologic system such as the Sahlenburg tidal flat area underscores the necessity for the integration of geological, geochemical, and geophysical based approaches to gain detailed information about carbon and nutrient cycles.

Data availability statement

The original contributions presented in the study are included in the article/Supplementary Material. All raw data will be made accessible in PANGAEA (https://pangaea.de/) after publication of the article.

Author contributions

HW and RSC conceived the study. All authors contributed to data interpretation. RSC wrote the manuscript with significant contributions from all authors. All authors contributed to the article and approved the submitted version.

Funding

This study was financed by MWK project "BIME" (ZN3184). RSC received a PhD scholarship funded by the Brazilian Ministry of Education agency (Coordenação de Aperfeiçoamento de Pessoal de Nível Superior, CAPES). Additional support was provided by the DFG through the marDOS Project (DI 842/6-1) and within the Cluster of Excellence EXC 2077 "The Ocean Floor – Earth's Uncharted Interface" (Project number 390741603). HW received funding from the DFG research unit "DynaDeep" (FOR 5094, WA 3067/3-1).

Acknowledgments

We thank Ina Ulber, Matthias Friebe, Katrin Klaproth, Carola Lehners, Heike Simon, Kai Schwalfenberg, Hanne Banko-Kubis and Linn Speidel for support with field work, sample analyses, data processing, and insightful discussions. Furthermore, we thank Gregor Scheiffarth from the National Park Authority Niedersachsen for his support with local conditions and permits.

Conflict of interest

The authors declare that the research was conducted in the absence of any commercial or financial relationships that could be construed as a potential conflict of interest.

Publisher's note

All claims expressed in this article are solely those of the authors and do not necessarily represent those of their affiliated organizations, or those of the publisher, the editors and the reviewers. Any product that may be evaluated in this article, or claim that may be made by its manufacturer, is not guaranteed or endorsed by the publisher.

Supplementary material

The Supplementary Material for this article can be found online at: https://www.frontiersin.org/articles/10.3389/fmars.2023.1128855/full#supplementary-material

References

Adyasari, D., Waska, H., Daehnke, K., Oehler, T., Pracoyo, A., Putra, D. P. E., et al. (2021). Terrestrial nutrients and dissolved organic matter input to the coral reef ecosystem *via* submarine springs. *ACS ES&T Water* 1, 1887–1900. doi: 10.1021/acsestwater.1c00134

Ahrens, J., Beck, M., Böning, P., Degenhardt, J., Pahnke, K., Schnetger, B., et al. (2021). Thallium cycling in pore waters of intertidal beach sediments. *Geochim. Cosmochim. Acta* 306, 321–339. doi: 10.1016/j.gca.2021.04.009

Ahrens, J., Beck, M., Marchant, H. K., Ahmerkamp, S., Schnetger, B., and Brumsack, H. J. (2020). Seasonality of organic matter degradation regulates nutrient and metal net fluxes in a high energy sandy beach. *J. Geophys. Res. Biogeosci.* 125, 1–21. doi: 10.1029/2019JG005399

Bartsch, S. (2009). *Erfassung von Porenwasservariationen in Wattsedimenten und der Einfluss von Grundwasseraustritt im Sahlenburger Watt*. Bremen: Geoscience, FB5, 178.

Beck, M., Dellwig, O., Holstein, J. M., Grunwald, M., Liebezeit, G., Schnetger, B., et al. (2008). Sulphate, dissolved organic carbon, nutrients and terminal metabolic products in deep pore waters of an intertidal flat. *Biogeochemistry* 89, 221–238. doi: 10.1007/s10533-008-9215-6

Beck, M., Reckhardt, A., Amelsberg, J., Bartholomä, A., Brumsack, H. J., Cypionka, H., et al. (2017). The drivers of biogeochemistry in beach ecosystems: A cross-shore transect from the dunes to the low-water line. *Mar. Chem.* 190, 35–50. doi: 10.1016/j.marchem.2017.01.001

Bishop, J. M., Glenn, C. R., Amato, D. W., and Dulai, H. (2017). Effect of land use and groundwater flow path on submarine groundwater discharge nutrient flux. *J. Hydrol. Reg. Stud.* 11, 194–218. doi: 10.1016/j.ejrh.2015.10.008

Brase, L., Bange, H. W., Lendt, R., Sanders, T., and Dähnke, K. (2017). High resolution measurements of nitrous oxide (N2O) in the Elbe estuary. *Front. Mar. Sci.* 4. doi: 10.3389/fmars.2017.00162

Burdige, D. J., and Gardner, K. G. (1998). Molecular weight distribution of dissolved organic carbon in marine sediment pore waters. *Mar. Chem.* 62, 45–64. doi: 10.1016/S0304-4203(98)00035-8

Burnett, W. C., Aggarwal, P. K., Aureli, A., Bokuniewicz, H., Cable, J. E., Charette, M. A., et al. (2006). Quantifying submarine groundwater discharge in the coastal zone *via* multiple methods. *Sci. Total Environ.* 367, 498–543. doi: 10.1016/j.scitotenv.2006.05.009

Buth, M., et al. (2015). Vulnerabilität Deutschlands gegenüber dem Klimawandel. Clim. Chang. 24, 2015.

Carruthers, T. J. B., van Tussenbroek, B. I., and Dennison, W. C. (2005). Influence of submarine springs and wastewater on nutrient dynamics of Caribbean seagrass meadows. *Estuar. Coast. Shelf Sci.* 64, 191–199. doi: 10.1016/j.ecss.2005.01.015

Coble, P. G. (1996). Characterization of marine and terrestrial DOM in seawater using excitation-emission matrix spectroscopy. *Mar. Chem.* 51, 325–346. doi: 10.1016/0304-4203(95)00062-3

Czitrom, S. P. R., Budéus, G., and Krause, G. (1988). A tidal mixing front in an area influenced by land runoff. *Cont. Shelf Res.* 8, 225–237. doi: 10.1016/0278-4343(88)90030-1

Danard, M. B., Dube, S. K., Gönnert, G., Munroe, A., Murty, T. S., Chittibabu, P., et al. (2004). Storm surges from extra-tropical cyclones. *Nat. Hazards* 32, 177–190. doi: 10.1023/B:NHAZ.0000031312.98231.81

D'Andrilli, J., Cooper, W. T., Foreman, C. M., and Marshall, A. G. (2015). An ultrahigh-resolution mass spectrometry index to estimate natural organic matter lability. *Rapid Communications in Mass Spectrometry*. 29 (24), 2385–2401.

Dittmar, T., Koch, B., Hertkorn, N., and Kattner, G. (2008). A simple and efficient method for the solid-phase extraction of dissolved organic matter (SPE-DOM) from seawater. *Limnol. Oceanogr. Methods* 6, 230–235. doi: 10.4319/lom.2008.6.230

Dittmar, T., Lennartz, S. T., Buck-Wiese, H., Hansell, D. A., Santinelli, C., Vanni, C., et al. (2021). Enigmatic persistence of dissolved organic matter in the ocean. *Nat. Rev. Earth Environ.* 2 (8), 570–583. doi: 10.1038/s43017-021-00183-7

Donis, D., Janssen, F., Liu, B., Wenzhöfer, F., Dellwig, O., Escher, P., et al. (2017). Biogeochemical impact of submarine ground water discharge on coastal surface sands of the southern Baltic Sea. *Estuar. Coast. Shelf Sci.* 189, 131–142. doi: 10.1016/j.ecss.2017.03.003

Flerus, R., Lechtenfeld, O. J., Koch, B. P., McCallister, S. L., Schmitt-Kopplin, P., Benner, R., et al. (2012). A molecular perspective on the ageing of marine dissolved organic matter. *Biogeosciences* 9, 1935–1955. doi: 10.5194/bg-9-1935-2012

Garcia, H. E., and Gordon, L. I. (1992). Oxygen solubility in seawater: Better fitting equations. *Limnology and oceanography*. 37 (6), 1307–1312.

Garcia-Solsona, E., Garcia-Orellana, J., Masqué, P., Rodellas, V., Mejías, M., Ballesteros, B., et al. (2010). Groundwater and nutrient discharge through karstic coastal springs (Castelló, Spain). *Biogeosciences* 7, 2625–2638. doi: 10.5194/bg-7-2625-2010

Goñi, M. A., and Gardner, I. R. (2003). Seasonal dynamics in dissolved organic carbon concentrations in a coastal water-table aquifer at the forest-marsh interface. *Aquat. Geochem.* 9, 209–232. doi: 10.1023/B:AQUA.0000022955.82700.ed

Gonsior, M., Peake, B. M., Cooper, W. T., Podgorski, D., D'Andrilli, J., and Cooper, W. J. (2009). Photochemically induced changes in dissolved organic matter identified by ultrahigh resolution fourier transform ion cyclotron resonance mass spectrometry. *Environ. Sci. Technol.* 43, 698–703. doi: 10.1021/es8022804

Hansen, H. P., and Koroleff, F. (2007). *Determination of nutrients, in: Methods of seawater analysis* (Weinheim, Germany: Wiley-VCH Verlag GmbH), 159–228. doi: 10.1002/9783527613984.ch10

Hays, R. L., and Ullman, W. J. (2007). Direct determination of total and fresh groundwater discharge and nutrient loads from a sandy beachface at low tide (Cape henlopen, Delaware). *Limnol. Oceanogr.* 52, 240–247. doi: 10.4319/lo.2007.52.1.0240

Hedges, J. I., Keil, R. G., and Benner, R. (1997). What happens to terrestrial organic matter in the ocean? *Org. Geochem.* 27, 195–212. doi: 10.1016/S0146-6380(97)00066-1

Holliday, D., Stieglitz, T. C., Ridd, P. V., and Read, W. W. (2007). Geological controls and tidal forcing of submarine groundwater discharge from a confined aquifer in a coastal sand dune system. *J. Geophys. Res.* 112, C04015. doi: 10.1029/2006JC003580

Ionita, M., and Nagavciuc, V. (2020). Forecasting low flow conditions months in advance through teleconnection patterns, with a special focus on summer 2018. *Sci. Rep.* 10, 13258. doi: 10.1038/s41598-020-70060-8

Itaya, K., and Ui, M. (1966). A new micromethod for the colorimetric determination of inorganic phosphate. *Clin. Chim. Acta* 14, 361–366. doi: 10.1016/0009-8981(66)90114-8

Jordan, T. E., Correll, D. L., and Weller, D. E. (1997). Relating nutrient discharges from watersheds to land use and streamflow variability. *Water resources research* 33 (11), 2579–2590.

Kalbus, E., Reinstorf, F., and Schirmer, M. (2006). Measuring methods for groundwater – surface water interactions: A review. *Hydrol. Earth Syst. Sci.* 10, 873–887. doi: 10.5194/hess-10-873-2006

Kim, G. (2003). Large Submarine groundwater discharge (SGD) from a volcanic island. *Geophys. Res. Lett.* 30, 2098. doi: 10.1029/2003GL018378

Kim, S., Kaplan, L. A., and Hatcher, P. G. (2006). Biodegradable dissolved organic matter in a temperate and a tropical stream determined from ultra-high resolution mass spectrometry. *Limnol. Oceanogr.* 51, 1054–1063. doi: 10.4319/lo.2006.51.2.1054

Kim, J., and Kim, G. (2017). Inputs of humic fluorescent dissolved organic matter *via* submarine groundwater discharge to coastal waters off a volcanic island (Jeju, Korea). *Sci. Rep.* 7 (1), 7921. doi: 10.1038/s41598-017-08518-5

Kim, T. H., Waska, H., Kwon, E., Suryaputra, I. G. N., and Kim, G. (2012). Production, degradation, and flux of dissolved organic matter in the subterranean estuary of a large tidal flat. *Mar. Chem.* 142–144, 1–10. doi: 10.1016/j.marchem.2012.08.002

Klages, S., Aue, C., Reiter, K., Heidecke, C., and Osterburg, B. (2022). Catch crops in lower Saxony–more than 30 years of action against water pollution with nitrates: All in vain? *Agriculture* 12, 447. doi: 10.3390/agriculture12040447

Koch, B. P., and Dittmar, T. (2016). From mass to structure: An aromaticity index for high-resolution mass data of natural organic matter. *Rapid Commun. Mass Spectrom.* 30, 250–250. doi: 10.1002/rcm.7433

Koch, B. P., Witt, M., Engbrodt, R., Dittmar, T., and Kattner, G. (2005). Molecular formulae of marine and terrigenous dissolved organic matter detected by electrospray ionization Fourier transform ion cyclotron resonance mass spectrometry. *Geochim. Cosmochim. Acta* 69, 3299–3308. doi: 10.1016/j.gca.2005.02.027

Kujawinski, E. B., Del Vecchio, R., Blough, N. V., Klein, G. C., and Marshall, A. G. (2004). Probing molecular-level transformations of dissolved organic matter: Insights on photochemical degradation and protozoan modification of DOM from electrospray ionization Fourier transform ion cyclotron resonance mass spectrometry. *Mar. Chem.* 92, 23–37. doi: 10.1016/j.marchem.2004.06.038

Laskov, C., Herzog, C., Lewandowski, J., and Hupfer, M. (2007). Miniaturized photometrical methods for the rapid analysis of phosphate, ammonium, ferrous iron, and sulfate in pore water of freshwater sediments. *Limnol. Oceanogr. Methods* 5, 63–71. doi: 10.4319/lom.2007.5.63

Linkhorst, A., Dittmar, T., and Waska, H. (2017). Molecular fractionation of dissolved organic matter in a shallow subterranean estuary: The role of the iron curtain. *Environ. Sci. Technol.* 51, 1312–1320. doi: 10.1021/acs.est.6b03608

Longnecker, K., and Kujawinski, E. B. (2011). Composition of dissolved organic matter in groundwater. *Geochim. Cosmochim. Acta* 75, 2752–2761. doi: 10.1016/j.gca.2011.02.020

Luzius, C., Guillemette, F., Podgorski, D. C., Kellerman, A. M., and Spencer, R. G. M. (2018). Drivers of dissolved organic matter in the vent and major conduits of the world's largest freshwater spring. *J. Geophys. Res. Biogeosci.* 123, 2775–2790. doi: 10.1029/2017JG004327

Manga, M. (2001). Using springs to study groundwater flow and active geologic processes. *Annu. Rev. Earth Planet. Sci.* 29, 201–228. doi: 10.1146/annurev.earth.29.1.201

Medeiros, P. M., Seidel, M., Niggemann, J., Spencer, R. G. M., Hernes, P. J., Yager, P. L., et al. (2016). A novel molecular approach for tracing terrigenous dissolved organic matter into the deep ocean. *Global Biogeochem. Cycles* 30, 689–699. doi: 10.1002/2015GB005320

Medeiros, P. M., Seidel, M., Ward, N. D., Carpenter, E. J., Gomes, H. R., Niggemann, J., et al. (2015). Fate of the Amazon river dissolved organic matter in the tropical Atlantic ocean. *Global Biogeochem. Cycles* 29, 677–690. doi: 10.1002/2015GB005115

Merder, J., Freund, J. A., Feudel, U., Hansen, C. T., Hawkes, J. A., Jacob, B., et al. (2020). ICBM-OCEAN: Processing ultrahigh-resolution mass spectrometry data of complex molecular mixtures. *Anal. Chem.* 92, 6832–6838. doi: 10.1021/acs.analchem.9b05659

Montiel, D., Lamore, A. F., Stewart, J., Lambert, W. J., Honeck, J., Lu, Y., et al. (2019). Natural groundwater nutrient fluxes exceed anthropogenic inputs in an ecologically impacted estuary: Lessons learned from mobile bay, Alabama. *Biogeochem* 145 (1), 1–33. doi: 10.1007/s10533-019-00587-0

Moore, W. S. (1999). The subterranean estuary: A reaction zone of ground water and sea water. *Mar. Chem.* 65, 111–125. doi: 10.1016/S0304-4203(99)00014-6

Moore, W. S., Blanton, J. O., and Joye, S. B. (2006). Estimates of flushing times, submarine groundwater discharge, and nutrient fluxes to okatee estuary, south Carolina. *J. Geophys. Res. Ocean.* 111, 1–14. doi: 10.1029/2005JC003041

Moore, W. S., Beck, M., Riedel, T., Van Der Loeff, M. R., Dellwig, O., Shaw, T. J., et al. (2011). Radium-based pore water fluxes of silica, alkalinity, manganese, DOC, and uranium: A decade of studies in the German Wadden Sea. *Geochimica et Cosmochimica Acta*. 75 (21), 6535–6555

Moosdorf, N., and Oehler, T. (2017). Societal use of fresh submarine groundwater discharge: An overlooked water resource. *Earth Sci. Rev.* 171, 338–348. doi: 10.1016/j.earscirev.2017.06.006

Moosdorf, N., Stieglitz, T., Waska, H., Dürr, H. H., and Hartmann, J. (2015). Submarine groundwater discharge from tropical islands: A review. *Grundwasser* 20, 53–67. doi: 10.1007/s00767-014-0275-3

Nebbioso, A., and Piccolo, A. (2013). Molecular characterization of dissolved organic matter (DOM): a critical review. *Anal. Bioanal. Chem.* 405, 109–124. doi: 10.1007/s00216-012-6363-2

Nelson, C. E., Donahue, M. J., Dulaiova, H., Goldberg, S. J., La Valle, F. F., Lubarsky, K., et al. (2015). Fluorescent dissolved organic matter as a multivariate biogeochemical tracer of submarine groundwater discharge in coral reef ecosystems. *Mar. Chem.* 177, 232–243. doi: 10.1016/j.marchem.2015.06.026

Null, K. A., Knee, K. L., Crook, E. D., de Sieyes, N. R., Rebolledo-Vieyra, M., Hernández-Terrones, L., et al. (2014). Composition and fluxes of submarine groundwater along the Caribbean coast of the Yucatan peninsula. *Cont. Shelf Res.* 77, 38–50. doi: 10.1016/j.csr.2014.01.011

Oehler, T., Eiche, E., Putra, D., Adyasari, D., Hennig, H., Mallast, U., et al. (2018). Seasonal variability of land-ocean groundwater nutrient fluxes from a tropical karstic region (southern Java, Indonesia). *J. Hydrol.* 565, 662–671. doi: 10.1016/j.jhydrol.2018.08.077

Oehler, T., Bakti, H., Lubis, R. F., Purwoarminta, A., Delinom, R., and Moosdorf, N. (2019a). Nutrient dynamics in submarine groundwater discharge through a coral reef (western lombok, Indonesia). *Limnol. Oceanogr.* 64, 2646–2661. doi: 10.1002/lno.11240

Oehler, T., Tamborski, J., Rahman, S., Moosdorf, N., Ahrens, J., Mori, C., et al. (2019b). DSi as a tracer for submarine groundwater discharge. *Front. Mar. Sci.* 6. doi: 10.3389/fmars.2019.00563

Osterholz, H., Dittmar, T., and Niggemann, J. (2014). Molecular evidence for rapid dissolved organic matter turnover in Arctic fjords. *Mar. Chem.* 160, 1–10. doi: 10.1016/j.marchem.2014.01.002

Osterholz, H., Kirchman, D. L., Niggemann, J., and Dittmar, T. (2016). Environmental drivers of dissolved organic matter molecular composition in the Delaware estuary. *Front. Earth Sci.* 4. doi: 10.3389/feart.2016.00095

Pain, A. J., Martin, J. B., Young, C. R., Huang, L., and Valle-Levinson, A. (2019). Organic matter quantity and quality across salinity gradients in conduit- vs. *Diffuse Flow Dominated Subterranean Estuaries Limnol. Oceanogr.* 64, 1386–1402. doi: 10.1002/lno.11122

Piotrowski, J. A. (1994). Tunnel-valley formation in northwest Germany-geology, mechanisms of formation and subglacial bed conditions for the Bornh6ved tunnel valley. *Sedimentary Geology*. 89 (1-2), 107–141.

Pohlabeln, A. M., Gomez-Saez, G. V., Noriega-Ortega, B. E., and Dittmar, T. (2017). Experimental evidence for abiotic sulfurization of marine dissolved organic matter. *Front. Mar. Sci.* 4. doi: 10.3389/fmars.2017.00364

Povinec, P. P. P., Bokuniewicz, H., Burnett, W. C. C., Cable, J., Charette, M., Comanducci, J.-F. F., et al. (2008). Isotope tracing of submarine groundwater discharge offshore ubatuba, Brazil: Results of the IAEA–UNESCO SGD project. *J. Environ. Radioact.* 99, 1596–1610. doi: 10.1016/j.jenvrad.2008.06.010

Rahman, M. A., González, E., Wiederhold, H., Deus, N., Elbracht, J., and Siemon, B. (2018). Characterization of a regional coastal zone aquifer using an interdisciplinary approach – an example from weser-Elbe region, lower Saxony, Germany. *E3S Web Conf.* 54, 26. doi: 10.1051/e3sconf/20185400026

Raymond, P. A., Saiers, J. E., and Sobczak, W. V. (2016). Hydological and biogeochemical controls on watershed dissolved organic matter transport: Pulse-shunt concept. *Ecology* 97, 5–16. doi: 10.1890/14-1684.1

R core team (2013). *R: A Language and Environment for Statistical Computing*. R foundation for statistical computing, Vienna, Austria. Available at: http://www.R-project.org/.

Reckhardt, A., Beck, M., Seidel, M., Riedel, T., Wehrmann, A., Bartholomä, A., et al. (2015). Carbon, nutrient and trace metal cycling in sandy sediments: A comparison of high-energy beaches and backbarrier tidal flats. *Estuar. Coast. Shelf Sci.* 159, 1–14. doi: 10.1016/j.ecss.2015.03.025

Reineck, H. E., and Siefert, W. (1980). Faktoren der Schlickbildung im Sahlenburger und Neuwerker Watt. *Die Küste* 35 (35), 26–51.

Repeta, D. J., Quan, T. M., Aluwihare, L. I., and Accardi, A. M. (2002). Chemical characterization of high molecular weight dissolved organic matter in fresh and marine waters. *Geochim. Cosmochim. Acta* 66, 955–962. doi: 10.1016/S0016-7037(01)00830-4

Riedel, T., and Dittmar, T. (2014). A method detection limit for the analysis of natural organic matter *via* Fourier transform ion cyclotron resonance mass spectrometry. *Anal. Chem.* 86, 8376–8382. doi: 10.1021/ac501946m

Rodemann, H., Brost, E., Schünemann, J., Noell, U., Siemon, B., and Binot, F. (2005). Gleichstromgeoelektrische untersuchungen eines mit aeroelektromagnetischen messungen kartierten süßwasservorkommens im sahlenburger watt unter berücksichtigung von Äquivalenzfällen und 2D/3D-modellrechnungen. *Z. fur Angew. Geol.* 1 (2005), 45–51.

Roebuck, J. A., Seidel, M., Dittmar, T., and Jaffé, R. (2019). Controls of land use and the river continuum concept on dissolved organic matter composition in an anthropogenically disturbed subtropical watershed. *Environ. Sci. Technol.* 54, acs.est.9b04605. doi: 10.1021/acs.est.9b04605

Röper, T., Greskowiak, J., and Massmann, G. (2014). Detecting small groundwater discharge springs using handheld thermal infrared imagery. *Groundwater* 52 (6), 936–942.

Santos, I. R., Bryan, K. R., Pilditch, C. A., and Tait, D. R. (2014). Influence of porewater exchange on nutrient dynamics in two new Zealand estuarine intertidal flats. *Mar. Chem.* 167, 57–70. doi: 10.1016/j.marchem.2014.04.006

Santos, I. R. S., Burnett, W. C., Chanton, J., Mwashote, B., Suryaputra, I. G. N. A., and Dittmar, T. (2008). Nutrient biogeochemistry in a gulf of Mexico subterranean estuary and groundwater-derived fluxes to the coastal ocean. *Limnol. Oceanogr.* 53, 705–718. doi: 10.4319/lo.2008.53.2.0705

Santos, I. R., Burnett, W. C., Dittmar, T., Suryaputra, I. G. N. A., and Chanton, J. (2009). Tidal pumping drives nutrient and dissolved organic matter dynamics in a gulf of Mexico subterranean estuary. *Geochim. Cosmochim. Acta* 73, 1325–1339. doi: 10.1016/j.gca.2008.11.029

Santos, I. R., Beck, M., Brumsack, H. J., Maher, D. T., Dittmar, T., Waska, H., et al. (2015). Porewater exchange as a driver of carbon dynamics across a terrestrial-marine transect: Insights from coupled 222Rn and pCO2 observations in the German Wadden Sea. *Marine Chemistry* 171, 10–20.

Santos, I. R., Chen, X., Lecher, A. L., Sawyer, A. H., Moosdorf, N., Rodellas, V., et al. (2021). Submarine groundwater discharge impacts on coastal nutrient biogeochemistry. *Nat. Rev. Earth Environ.* 2, 307–323. doi: 10.1038/s43017-021-00152-0

Santos, I. R., Eyre, B. D., and Huettel, M. (2012). The driving forces of porewater and groundwater flow in permeable coastal sediments: A review. *Estuar. Coast. Shelf Sci.* 98, 1–15. doi: 10.1016/j.ecss.2011.10.024

Schlüter, M., and Maier, P. (2021). Submarine groundwater discharge from sediments and sand boils quantified by the mean residence time of a tracer injection. *Front. Earth Sci.* 9. doi: 10.3389/feart.2021.710000

Schlüter, M., Sauter, E. J., Andersen, C. E., Dahlgaard, H., and Dando, P. R. (2004). Spatial distribution and budget for submarine groundwater discharge in eckernförde bay (Western Baltic Sea). *Limnol. Oceanogr.* 49 (1), 157–167. doi: 10.4319/lo.2004.49.1.0157

Schmidt, F., Elvert, M., Koch, B. P., Witt, M., and Hinrichs, K. U. (2009). Molecular characterization of dissolved organic matter in pore water of continental shelf sediments. *Geochim. Cosmochim. Acta* 73, 3337–3358. doi: 10.1016/j.gca.2009.03.008

Schmidt, C., Hanfland, C., Regnier, P., Van Cappellen, P., Schlüter, M., Knauthe, U., et al. (2011). 228Ra, 226Ra, 224Ra and 223Ra in potential sources and sinks of land-derived material in the German bight of the north Sea: Implications for the use of radium as a tracer. *Geo Marine Lett.* 31, 259–269. doi: 10.1007/s00367-011-0231-5

Schnetger, B., and Lehners, C. (2014). Determination of nitrate plus nitrite in small volume marine water samples using vanadium(III)chloride as a reduction agent. *Mar. Chem.* 160, 91–98. doi: 10.1016/j.marchem.2014.01.010

Seeberg-Elverfeldt, J., Schlüter, M., Feseker, T., and Kölling, M. (2005). Rhizon sampling of pore waters near the sediment/water interface of aquatic systems. *Limnol. Oceanogr. Methods* 3, 361–371. doi: 10.4319/lom.2005.3.361

Seidel, M., Beck, M., Greskowiak, J., Riedel, T., Waska, H., Suryaputra, I. G. N. A., et al. (2015). Benthic-pelagic coupling of nutrients and dissolved organic matter composition in an intertidal sandy beach. *Mar. Chem.* 176, 150–163. doi: 10.1016/j.marchem.2015.08.011

Seidel, M., Beck, M., Riedel, T., Waska, H., Suryaputra, I. G. N. A., Schnetger, B., et al. (2014). Biogeochemistry of dissolved organic matter in an anoxic intertidal creek bank. *Geochim. Cosmochim. Acta* 140, 418–434. doi: 10.1016/j.gca.2014.05.038

Seidel, M., Manecki, M., Herlemann, D. P. R., Deutsch, B., Schulz-Bull, D., Jürgens, K., et al. (2017). Composition and transformation of dissolved organic matter in the Baltic sea. *Front. Earth Sci.* 5. doi: 10.3389/feart.2017.00031

Shen, Y., Chapelle, F. H., Strom, E. W., and Benner, R. (2015). Origins and bioavailability of dissolved organic matter in groundwater. *Biogeochemistry* 122, 61–78. doi: 10.1007/s10533-014-0029-4

Slomp, C. P., and Van Cappellen, P. (2004). Nutrient inputs to the coastal ocean through submarine groundwater discharge: Controls and potential impact. *J. Hydrol.* 295, 64–86. doi: 10.1016/j.jhydrol.2004.02.018

Smith, A. M., and Cave, R. R. (2012). Influence of fresh water, nutrients and DOC in two submarine-groundwater-fed estuaries on the west of Ireland. *Sci. Total Environ.* 438, 260–270. doi: 10.1016/j.scitotenv.2012.07.094

Stedmon, C. A., Markager, S., and Bro, R. (2003). Tracing dissolved organic matter in aquatic environments using a new approach to fluorescence spectroscopy. *Mar. Chem.* 82, 239–254. doi: 10.1016/S0304-4203(03)00072-0

Steen, A. D., Kusch, S., Abdulla, H. A., Cakić, N., Coffinet, S., Dittmar, T., et al (2020). Analytical and computational advances, opportunities, and challenges in marine organic biogeochemistry in an era of "Omics". *Front. Mar. Sci.* 7. doi: 10.3389/fmars.2020.00718

Sterr, H. (2008). Assessment of vulnerability and adaptation to Sea-level rise for the coastal zone of Germany. *J. Coast. Res.* 242, 380–393. doi: 10.2112/07A-0011.1

Steuer, A., Siemon, B., and Auken, E. (2009). A comparison of helicopter-borne electromagnetics in frequency- and time-domain at the cuxhaven valley in northern Germany. *J. Appl. Geophys.* 67, 194–205. doi: 10.1016/j.jappgeo.2007.07.001

Stubbins, A., Lapierre, J. F., Berggren, M., Prairie, Y. T., Dittmar, T., del Giorgio, P. A., et al. (2014). What's in an EEM? Molecular signatures associated with dissolved organic fluorescence in boreal Canada. *Environmental science & technology*. 48 (18), 10598–10606.

Streif, H. (2002). "The Pleistocene and Holocene development of the southeastern North Sea basin and adjacent coastal areas," in *Climate Development and History of the North Atlantic Realm*, eds G. Wefer, W. Berger, K.-E. Behre and E. Jansen (Berlin: Springer), 387–397. doi: 10.1007/978-3-662-04965-5_25

Swarzenski, P. W., Dulai, H., Kroeger, K. D., Smith, C. G., Dimova, N., Storlazzi, C. D., et al. (2017). Observations of nearshore groundwater discharge: Kahekili beach park submarine springs, Maui, Hawaii. *J. Hydrol. Reg. Stud.* 11, 147–165. doi: 10.1016/j.ejrh.2015.12.056

Szymczycha, B., Maciejewska, A., Winogradow, A., and Pempkowiak, J. (2014). Could submarine groundwater discharge be a significant carbon source to the southern Baltic Sea? *Oceanologia* 56, 327–347. doi: 10.5697/oc.56-2.327

Tamborski, J., van Beek, P., Conan, P., Pujo-Pay, M., Odobel, C., Ghiglione, J.-F., et al. (2020). Submarine karstic springs as a source of nutrients and bioactive trace metals for the oligotrophic Northwest Mediterranean Sea. *Sci. Total Environ.* 732, 139106. doi: 10.1016/j.scitotenv.2020.139106

Tiemeyer, B., Pfaffner, N., Frank, S., Kaiser, K., and Fiedler, S. (2017). Pore water velocity and ionic strength effects on DOC release from peat-sand mixtures: Results from laboratory and field experiments. *Geoderma* 296, 86–97. doi: 10.1016/j.geoderma.2017.02.024

Toth, J. (1971). Groundwater discharge: A common generator of diverse geologic and morphologic phenomena. *Int. Assoc. Sci. Hydrol. Bull.* 16, 7–24. doi: 10.1080/02626667109493029

Toth, D. J., and Katz, B. G. (2006). Mixing of shallow and deep groundwater as indicated by the chemistry and age of karstic springs. *Hydrogeol. J.* 14, 827–847. doi: 10.1007/s10040-005-0478-x

Viollier, E., Inglett, P. W., Hunter, K., Roychoudhury, A. N., and Cappellen, P.V. (2000). The ferrozine method revisted. *Appl. Geochem.* 15, 785–790. doi: 10.1016/S0883-2927(99)00097-9

Wagner, S., Schubotz, F., Kaiser, K., Hallmann, C., Waska, H., Rossel, P. E., et al. (2020). Soothsaying DOM: A current perspective on the future of oceanic dissolved organic carbon. *Front. Mar. Sci.* 7. doi: 10.3389/fmars.2020.00341

Waska, H., Brumsack, H. J. J., Massmann, G., Koschinsky, A., Schnetger, B., Simon, H., et al. (2019). Inorganic and organic iron and copper species of the subterranean estuary: Origins and fate. *Geochim. Cosmochim. Acta* 259, 211–232. doi: 10.1016/j.gca.2019.06.004

Waska, H., and Kim, G. (2010). Differences in microphytobenthos and macrofaunal abundances associated with groundwater discharge in the intertidal zone. *Mar. Ecol. Prog. Ser.* 407, 159–172. doi: 10.3354/meps08568

Waska, H., Simon, H., Ahmerkamp, S., Greskowiak, J., Ahrens, J., Seibert, S. L., et al. (2021). Molecular traits of dissolved organic matter in the subterranean estuary of a high-energy beach: Indications of sources and sinks. *Front. Mar. Sci.* 8. doi: 10.3389/fmars.2021.607083

Webb, J. R., Santos, I. R., Maher, D. T., Tait, D. R., Cyronak, T., Sadat-Noori, M., et al. (2019). Groundwater as a source of dissolved organic matter to coastal waters: Insights from radon and CDOM observations in 12 shallow coastal systems. *Limnol. Oceanogr.* 64, 182–196. doi: 10.1002/lno.11028

Welskel, P. K., and Howes, B. L. (1992). Differential transport of sewage-derived nitrogen and phosphorus through a coastal watershed. *Environ. Sci. Technol.* 26, 352–360. doi: 10.1021/es00026a017

Zark, M., and Dittmar, T. (2018). Universal molecular structures in natural dissolved organic matter. *Nat. Commun.* 9, 1–8. doi: 10.1038/s41467-018-05665-9

Zipperle, A., and Reise, K. (2005). Freshwater springs on intertidal sand flats cause a switch in dominance among polychaete worms. *J. Sea Res.* 54, 143–150. doi: 10.1016/j.seares.2005.01.003